Performance of Molecular Orbital Methods and Density Functional Theory in the Computation of Geometries and Energies of Metal Aqua Ions

François P. Rotzinger*

Ecole Polytechnique Fédérale, Institut des Sciences et Ingénierie Chimiques, Station 6, CH-1015 Lausanne, Switzerland

Received: October 8, 2004

Geometries and energies of various metal aqua ions have been computed with Hartree−Fock (HF), single-reference second-order perturbation theory according to Møller and Plesset (MP2), complete active space self-consistent field (CAS−SCF) methods, multi-configurational quasi-degenerate second-order perturbation theory (MCQDPT2), and density functional theory (DFT), whereby for the latter the most widely used functionals BLYP, B3LYP, LDA ("local density approximation"), and another functional (SOP) exhibiting Slater exchange, have been investigated. The geometries as well as the energies are sensitive to the computational method, results of which can lead to different conclusions. The geometries of certain reactants, products, intermediates, or transition states cannot be obtained with all of the above-mentioned computational methods: in some cases, the structures are very poor, exhibiting large errors in the bond parameters, and in others, the targeted species cannot be calculated at all. The different computational techniques do not always predict the same coordination number of a given aqua ion or the same preferred water exchange mechanism. Inaccuracies arising from inadequate basis sets are also discussed.

Introduction

The choice of a quantum chemical method for the computation of a physical property is based on the property of interest itself and on the size of the system. In situations where the application of several methods can be envisaged, quite often the computational technique is selected arbitrarily. In some cases, the choice is not critical, whereas in others, the result depends strongly on the method, and so do the conclusions.

For organometallic compounds, the influence of the basis set and the computational method on the structure, reaction, or activation energies was investigated in earlier studies.[1−7] The requirements for the basis sets of transition metals were analyzed, in particular those for the valence *n*d shell and the formally empty (*n*+1)s and (*n*+1)p shells, being involved in metal−ligand bonding.[1,2]

In systems with static electron correlation, which may arise from the d manifold of a transition metal or from an elongated bond, in which the bonding (occupied) molecular orbital (MO) is close to its antibonding (unoccupied) counterpart, methods based on a single reference such as Hartree−Fock (HF), single-reference configuration interaction (CI), or perturbation theory are inadequate.[2−5] Also in those cases, where the description of correlation requires "excitations" of more than two electrons, single-reference methods involving the excitation of at the most two electrons such as second-order perturbation theory according to Møller and Plesset (MP2)[8] or singles-doubles configuration interaction (SDCI),[9] are inappropriate.[5,6] In 1996, the methods for the computation of electron correlation were reviewed.[10] Meanwhile, second-order perturbation theory based on a complete active space self-consistent field (CAS−SCF)[11] wave function, for example CASPT2[12,13] or MCQDPT2,[14,15] starts to become practicable for geometry optimizations. Today, for systems such as those treated in the present study, these are the best and most efficient techniques for the computation of electron correlation.

Metal aqua ions are chemically, and also computationally, quite different from organometallic compounds. High oxidation states are common for aqua, hydroxo, and especially oxo ions, while in organometallic complexes, low oxidation states prevail. In these two classes of compounds, metal-to-ligand bonding is also different: in general, the low oxidation states are stabilized by back-bonding, whereas the high oxidation states are stabilized by the lone pairs of water, hydroxide, or oxide ligands. Furthermore, H-bonding has to be described correctly. Water exchange reactions[16,17] of transition metal aqua ions have been investigated with HF, CAS−SCF, and density functional theory (DFT). In certain cases, these methods gave rise to different results and interpretations, and this calls for the assessment of the accuracy of the currently used computational techniques. Thus, the present study focuses on the accuracy of geometries and energies of metal aqua ions, computed with ab initio molecular orbital (MO) methods and DFT. The geometry and the energy are the most important quantities for the determination of coordination numbers of aqua ions and for the study of their reaction mechanisms as well. HF, CAS−SCF, MP2, multireference quasi-degenerate second-order perturbation theory (MCQDPT2), as well as the most widely used functionals are investigated. All of these calculations are performed for the free ions in the gas phase, and the accuracy of the geometry and energy is assessed. Computations including solvation are also discussed briefly. Two review articles on the water exchange mechanisms of metal aqua complexes are available,[16,17] the first one dealing with experiments and simulations, and the second one discussing classical, semiempirical, and quantum chemical methods.

* E-mail: francois.rotzinger@epfl.ch. Fax ++41 21 693 41 11.

10.1021/jp045407v CCC: $30.25
Published on Web 01/08/2005

For the computation of thermochemical data, multicoefficient methods[18−20] such as, for example, G3, MCCM, or SAC are developed. They are designed to yield a maximum accuracy at minimum computational labor by combining various techniques using empirical coefficients. The present study is not intended to supply the highest possible accuracy in the most efficient way, but rather to show, how methods such as HF, CAS−SCF, MP2, MCQDPT2, and DFT based on the most widely applied functionals perform, and how the technique that produces reliable results can be found in a systematic manner. It is indispensable to treat electron correlation adequately. In particular, its nature, dynamic or static *and* dynamic, has to be determined. It depends on the occupation of the valence d shell of the metal ion and on its ligands as well. Thus, in similar compounds, electron correlation can be quite different and consequently, the calculated properties, geometry, and energy, for example, will depend on the computational method. Thus, to obtain reliable properties, electron correlation needs to be treated correctly; although in certain cases, less demanding methods can produce acceptable results, their reliability has to be assessed via comparisons with an accurate method. For representative basis sets, the basis set superposition error (BSSE) is determined, showing that all-electron basis sets exhibit large BSSEs that increase with increasing charge on the metal ion, unless the basis sets are adapted to the system by adding and/or uncontracting functions.

Today, many studies are devoted to the computation of properties and reactions of species in solution. Since such calculations are demanding as the computational resources are concerned, medium-size basis sets have been used, although for many of the present examples, larger basis sets could have been taken. It will be shown that, if the BSSE is kept small, the size of the basis set, which in general should be of the split-valence + polarization quality at least, is less critical than the computational method.

Computational Details

All of the calculations were performed using the GAMESS[21] programs. Unless noted otherwise, the basis sets of Stevens, Basch, Krauss, and Jasien (SBKJ)[22] were used for the transition metals, where the inner shells are represented by relativistic effective core potentials (ECPs), the valence and the semi-core s and p shells have double-ζ and the valence d shell triple-ζ quality. For C, O, and H, 6-31G(d) or 6-311G(d,p) basis sets[23−25] were used ($\alpha_d = 0.80$ and 1.20, $\alpha_p = 0.80$,[26] respectively). For Ca, the ECP basis set of Wadt and Hay[27] with or without a d polarization function ($\alpha_d = 0.15$) was taken. In some cases, anion diffuse functions were added to the 6-31G(d) and 6-311G(d,p) basis sets, whereby the exponents were calculated as described by Giordan and Custodio.[28] For the high-valent aqua ions of VO^{2+}, calculations were also performed with SBKJ basis sets, in which either the outermost primitive of the 3d and 3sp functions (SBKJu), or one 3d and two 3sp functions (SBKJu2) were uncontracted.

The Hessians were calculated analytically, or numerically using the double-difference method and projected to eliminate rotational and translational contaminants.[29] The HF and DFT calculations on open-shell systems were performed at the restricted open shell level, whereas the (single reference) MP2 computations were done at the unrestricted level. A finer grid than the default was used for the DFT calculations (NTHE = 24 and NPHI = 48; the default is NTHE = 12 and NPHI = 24). The computed vibrational spectrum of transition states exhibited a single imaginary frequency, whereas for the other species, all of the calculated frequencies were real.

The geometry optimizations at the MCQDPT2 level were performed using numerical gradients.

Results

Electron Correlation. Treatment of electron correlation with an appropriate technique is a requirement to obtain accurate properties. In certain cases, correlation can be treated with simple methods or even neglected, but the validity of such approximations must always be assessed. To find an adequate computational method, the nature of the electron correlation, dynamic or static and dynamic, needs to be elucidated. This can be done in a systematic manner by performing multireference singles-doubles CI calculations (MR−SDCI). Because even for the present systems, especially those with unpaired electrons in the d shell, the number of configuration state functions or determinants is too large, one has to resort to the iterative natural orbital method (INO).[30] In general, solely dynamic electron correlation is present, if the natural orbitals (NO) have occupations close to 2, 1, and 0, whereas NO occupations deviating considerably from 2, 1, or 0 indicate the presence of static correlation. Usually, these NOs constitute the active space of the CAS−SCF wave function. It should be noted, however, that it is not always easy to find out which NOs need to be included in the active space of the CAS−SCF wave function, and which ones not: a series of CAS−CI or CAS−SCF calculations on possible active spaces might be helpful. In some cases, the MCQDPT2 energies depend strongly on the CAS−SCF active space and, furthermore, errors may arise from intruder states.[31] If only dynamic correlation is present, MP2 is appropriate. Otherwise, the MCQDPT2 method (or other second-order perturbation techniques based on CAS−SCF) is required. Instead of the rather demanding MR−SDCI technique, the recently developed occupation-restricted multiple active space (ORMAS) CI method[32] of Ivanic can be used. Thus, the MR−SDCI or ORMAS−CI calculations are used for the determination of the active space of the CAS−SCF wave function, and the properties are evaluated with MCQDPT2. As already mentioned, for the present systems, that are of a modest size, a single MR−SDCI or ORMAS−CI calculation on the entire system is not feasible or prohibitive. For all of the ions described in the following, this procedure has been used for the elucidation of the nature of electron correlation.

It is worthwhile to note that the presence of static electron correlation can show up in the unavailability of the MP2 gradient.

Geometry of Aqua Ions. *(i) Water Adducts of Hexaaqua Ions, $M(OH_2)_6 \cdot OH_2^{n+}$.* A simple model[33,34] for the computation of the associative (**A**) and interchange (**I_a**, **I**, **I_d**) water exchange mechanisms on transition metal hexaaqua ions involves the adduct of the reactant with one H_2O in the second coordination sphere, $M(OH_2)_6 \cdot OH_2^{n+}$. The isomer in which the seventh H_2O forms two H-bonds with two H_2Os of the first coordination sphere is more stable than that exhibiting a single H-bond (Figure 1).[35−37] The geometry of the latter isomer, in particular the M−O (d_0), the O−H_A (d_1), and $H_A \cdots$O (d_2) bond lengths (Figure 2), are quite sensitive to the computational method.

In the first set of $M(OH_2)_6 \cdot OH_2^{n+}$ complexes (Figure 1) exhibiting C_s symmetry, static electron correlation is absent because transition metal ions with an empty (Sc^{III}), a half-filled (Mn^{II} and Fe^{III}), or a filled (Zn^{II}) 3d shell are chosen. For these compounds, the MP2 method can be considered as the most accurate available technique. Thus, the geometry is optimized with HF, MP2, the widely used BLYP[38−40] and B3LYP[41−43] functionals, the local density approximation (LDA) with Slater

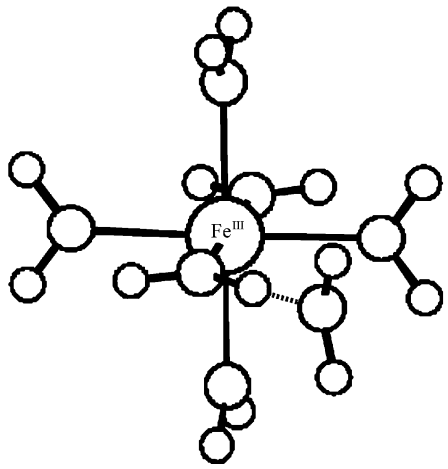

Figure 1. Perspective view of the $Fe(OH_2)_6 \cdot OH_2^{3+}$ ion with C_s symmetry (MP2 geometry).

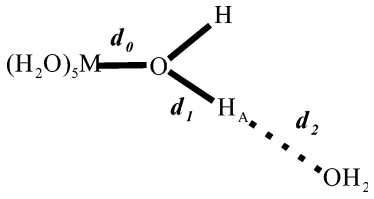

Figure 2. Schematic representation of the bond lengths of interest in $M(OH_2)_6 \cdot OH_2^{n+}$ or $MOH(OH_2)_5 \cdot H_3O^{n+}$ species.

exchange[44] and Vosko-Wilk-Nusair correlation[45] (SVWN), and the SOP[44,46,47] functional that involves also the Slater exchange. The most sensitive bond parameters, d_0, d_1, and d_2 (Figure 2) are summarized in Table 1.

The results are compared with MP2. In general, the HF values deviate with a sign opposite from those of DFT, whereas their (absolute) magnitude is similar for HF, BLYP, and B3LYP, but larger for the functionals with Slater exchange,[44] SVWN and SOP, which are inferior to the functionals with Becke exchange.

In the trivalent ions, there is a pronounced difference between DFT and the ab initio molecular orbital (MO) methods: with DFT, the H_A proton (Figure 2) is transferred "spontaneously" to the H_2O in the second coordination sphere, yielding $MOH(OH_2)_5 \cdot H_3O^{3+}$ species (M = Sc^{III} and Fe^{III}). This is observed for all four investigated functionals (it was not possible to obtain the geometry of $M(OH_2)_6 \cdot OH_2^{3+}$ species with DFT). This limitation is not due to the basis set because virtually identical geometries are obtained with 6-311G(d,p) basis sets for O and H (see below). In contrast, the geometries of both species, the aqua ions $M(OH_2)_6 \cdot OH_2^{3+}$ as well as their corresponding deprotonated species, $MOH(OH_2)_5 \cdot H_3O^{3+}$ (M = Sc^{III} and Fe^{III}), are obtained with HF and MP2. The geometry of the Sc^{III} species calculated via the two functionals with Slater exchange (SVWN and SOP) in fact corresponds neither to $Sc(OH_2)_6 \cdot OH_2^{3+}$ nor to $ScOH(OH_2)_5 \cdot H_3O^{3+}$, but rather to $Sc(OH_2)_5O(H)\cdots H\cdots OH_2^{3+}$, since H_A (Figure 2) is located approximately in the center between the two oxygen atoms (Table 1).

The aqua ion of V^{III} is particularly interesting because in this high-spin d^2 system, there is static electron correlation as revealed by multireference singles-doubles configuration interaction (MR−SDCI) computations using the iterative natural orbital method (INO).[30] A "state-of-the-art" calculation thus requires the treatment of both, static and dynamic electron correlation, which is realized on the basis of the MCQDPT2 method.

Again, as for Sc^{III} and Fe^{III}, the geometry of the nondeprotonated species, $V(OH_2)_6 \cdot OH_2^{3+}$, cannot be obtained with DFT

TABLE 1: Selected Bond Lengths in $M(OH_2)_6 \cdot OH_2^{n+}$ Complexes (M = Sc^{III}, Mn^{II}, Fe^{III}, and Zn^{II})

method	d_0, Å[a]	d_1, Å[a]	d_2, Å[a]
	(i) Sc^{III}		
HF	2.114 (+), 2.003 (−) [b]	1.006 (- -), 1.524 (+++) [b]	1.559 (+++), 1.027 (- -) [b]
MP2	**2.094**, **2.018** [b]	**1.068**, **1.420** [b]	**1.437**, **1.087** [b]
BLYP	2.014 [b]	1.389 (- -) [b]	1.122 (++) [b]
B3LYP	2.007 (−) [b]	1.345 (- -) [b]	1.127 (++) [b]
SVWN[c]	1.992 (−) [b]	1.248 (- - -) [b]	1.185 (++) [b]
SOP	1.997 (−) [b]	1.275 (- - -) [b]	1.174 (++) [b]
	(ii) Mn^{II}		
HF	2.183 (++)	0.968 (−)	1.736 (++)
MP2	**2.150**	**0.995**	**1.669**
BLYP	2.136 (−)	1.023 (+)	1.600 (- -)
B3LYP	2.135 (−)	1.007 (+)	1.610 (- -)
SVWN[c]	2.057 (- -)	1.027 (++)	1.543 (- - -)
SOP	2.067 (- -)	1.033 (++)	1.552 (- - -)
	(iii) Fe^{III}		
HF	1.991 (++), 1.896 [b]	1.012 (- -), 1.570 (++) [b]	1.538 (+++), 1.016 (- -) [b]
MP2	**1.955**, **1.890** [b]	**1.099**, **1.524** [b]	**1.369**, **1.049** [b]
BLYP	1.930 (++) [b,d]	1.533 [b,d]	1.070 (+) [b,d]
B3LYP	1.895 [b]	1.517 [b]	1.056 [b]
SVWN[c]	1.893 [b]	1.317 (- - -) [b]	1.137 (++) [b]
SOP	1.901 (+) [b]	1.330 (- - -) [b]	1.140 (++) [b]
	(iv) Zn^{II}		
HF	2.072 (+)	0.968 (−)	1.727 (++)
MP2	**2.045**	**0.995**	**1.666**
BLYP	2.054	1.022 (+)	1.602 (- -)
B3LYP	2.043	1.006 (+)	1.609 (- -)
SVWN[c]	1.976 (- -)	1.026 (++)	1.538 (- - -)
SOP	1.984 (- -)	1.032 (++)	1.547 (- - -)

[a] In parentheses: deviations from the corresponding MP2 value (+/−: 0.01−0.03 Å, ++/- -: >0.03 Å, +++/- - -: >0.10 Å). [b] Deprotonated species, $MOH(OH_2)_5 \cdot H_3O^{3+}$ (M = Sc or Fe). [c] Local density approximation. [d] The same geometry has been obtained starting from $Fe(OH_2)_6 \cdot OH_2^{3+}$ (HF) as well as $FeOH(OH_2)_5 \cdot H_3O^{3+}$ (HF).

TABLE 2: Selected Bond Lengths in $V(OH_2)_6 \cdot OH_2^{3+}$ and $VOH(OH_2)_5 \cdot H_3O^{3+}$ Complexes

method	d_0, Å	d_1, Å	d_2, Å
	(i) $V(OH_2)_6 \cdot OH_2^{3+}$		
HF	1.986, 1.980[a] (2.046, [b] 2.028)[c]	1.016, 1.025[a] (1.000, [b] 1.010)[c]	1.523, 1.470[a] (1.579, [b] 1.544)[c]
CAS−SCF[d]	1.995, 1.988[a]	1.014, 1.022[a]	1.529, 1.477[a]
MCQDPT2[d]	**1.942**	**1.143**	**1.305**
MP2	1.971, 1.966[a]	1.093, 1.052[a]	1.381, 1.445[a]
	(ii) $VOH(OH_2)_5 \cdot H_3O^{3+}$		
HF	1.897, 1.896[a]	1.601, 1.601[a]	1.010, 1.005[a]
CAS−SCF	1.902,[d] 1.908[e] 1.902,[a,d] 1.908[a,e]	1.595,[d] 1.711[e] 1.590,[a,d] 1.748[a,e]	1.011,[d] 0.994 [e] 1.007,[a,d] 0.987[a,e]
MCQDPT2	**1.890**,[d] **1.895** [e]	**1.586**,[d] **1.627** [e]	**1.035**,[d] **1.026** [e]
MP2	*f*	*f*	*f*
BLYP	1.906, 1.907[a]	1.517, 1.531[a]	1.074, 1.062[a]
B3LYP	1.890, [g] 1.891[a,g]	1.497, [g] 1.497[a,g]	1.062, [g] 1.055[a,g]
SVWN [h]	1.873	1.318	1.136
SOP	1.882	1.332	1.140

[a] 6-311G(d,p) basis set for O and H. [b] Transition state (exhibiting one imaginary frequency). [c] d_i for the two other (excited) d_π^2 states. [d] Active space: 2 electrons in 4 orbitals. [e] Active space: 8 electrons in 8 orbitals. [f] For the deprotonated species, the geometry optimization at the MP2 level is not possible because of static electron correlation. [g] This geometry has been obtained starting from $V(OH_2)_6 \cdot OH_2^{3+}$ (HF) as well as $VOH(OH_2)_5 \cdot H_3O^{3+}$ (HF). [h] Local density approximation.

(Table 2). Virtually identical geometries are obtained with HF and CAS−SCF, which could suggest, perhaps erroneously, that the geometry is insensitive to static correlation. Comparison of the MP2 and MCQDPT2 bond lengths, computed with the smaller basis set, shows that, once dynamic electron correlation

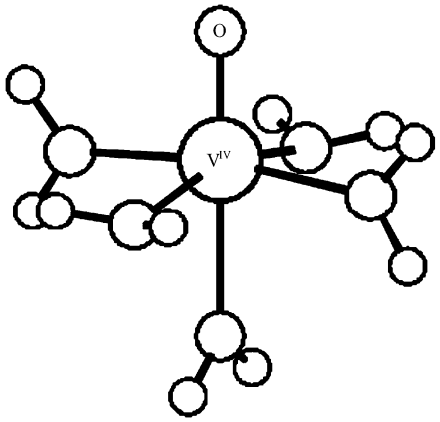

Figure 3. Perspective view of the $VO(OH_2)_5^{2+}$ ion with C_{2v} symmetry (MCQDPT2 geometry).

is treated, static correlation has a modest effect on d_0, d_1, and d_2. It should be noted that the HF, CAS−SCF, and MP2 geometries are quite similar for the larger basis set, for which the corresponding MCQDPT2 computations are prohibitive (yet). Static electron correlation has, if at all, a modest influence on d_0, d_1, and d_2.

In the deprotonated species, $VOH(OH_2)_5{\cdot}H_3O^{3+}$, the V−OH bond ($d_0$) is shorter by at least 0.05 Å than the V−OH_2 bonds. Static electron correlation is stronger and, for this reason, MP2 geometry optimizations are not feasible (Table 2). The MR−SDCI calculations suggest that the three lone pairs of the OH^- ligand might need to be included in the active space, and therefore the CAS−SCF and MCQDPT2 computations are performed on the basis of two active spaces. For all of the ab initio MO methods and the functionals with Becke exchange, equal d_0 values are obtained. As in the previous examples, DFT produces shorter d_1 and longer d_2 data, which is considerably worse for the functionals with Slater exchange. It should be noted that, at the CAS−SCF level, the larger active space gives rise to a longer d_1, whereas with MCQDPT2, this increase is much smaller, whereby the geometry is quite insensitive to the size of the active space of the CAS−SCF wave function. Obviously, the selection of the active space for CAS−SCF is by no means straightforward because, in certain cases, it may be difficult to distinguish static from dynamic correlation. Also for the deprotonated $VOH(OH_2)_5{\cdot}H_3O^{3+}$ species, static electron correlation has a weak influence on the geometry.

(ii) $VO(OH_2)_5^{2+}$ Ion and Its Water Adduct $VO(OH_2)_5{\cdot}OH_2^{2+}$. ORMAS−CI calculations on $VO(OH_2)_5^{2+}$, exhibiting C_{2v} symmetry, (Figure 3) indicated the presence of static electron correlation, which is the cause of the unavailability of MP2 geometries. A "state-of-the-art" calculation requires a method such as second-order perturbation theory based on a CAS−SCF wave function, which was realized using the MCQDPT2 technique. The V═O and the V−O bonds cis to V═O are insensitive to the basis set, but depend strongly on the computational method (Table 3). As it will be shown in the "Basis Set Superposition Error (BSSE)" section, for high-valent metal ions, the uncontraction of one d and one semi-core s/p function might be advisable. In the present case, the uncontractions have no effect on the V═O and cis V−O bonds, whereas the trans V−O bond is elongated slightly. With respect to MCQDPT2, all of the methods yield too short V═O bonds, whereby the error is unacceptably large for HF. The functionals with Becke exchange produce good V−O bonds which, however, are too short for the functionals with Slater exchange. Interestingly, for the V−O bonds, CAS−SCF is slightly less accurate than BLYP and B3LYP.

For the water adduct $VO(OH_2)_5{\cdot}OH_2^{2+}$, several isomers exist. That with C_s symmetry (Figure 4), resembling most closely the $M(OH_2)_6{\cdot}OH_2^{n+}$ ions, has been computed. (In the other isomers, the water in the second coordination sphere interacts with the V═O fragment). For the V═O and V−O bonds (Table 4), the performance of the various methods is as for $VO(OH_2)_5^{2+}$ (Table 3). With respect to HF and CAS−SCF, DFT produces too long O−H bonds (d_1). As for the $M(OH_2)_6{\cdot}OH_2^{2+}$ species, DFT yields a shorter H-bond (d_2) with the water molecule in the second sphere than do HF and CAS−SCF.

The investigation of the water exchange mechanism on $VO(OH_2)_5^{2+}$ would require MCQDPT2 energies based on CAS−SCF and BLYP or B3LYP geometries, whereby hydration needs to be included. The two types of geometries (CAS−SCF and B(3)LYP), exhibiting different errors, might give indications on the effect of the inaccurate V−O, O−H, and H···O bond lengths on the energy. Quite obviously, the computations on $VO(OH_2)_5^{2+}$ in aqueous solution are a demanding task. The water adducts $M(OH_2)_6{\cdot}OH_2^{n+}$ ($n = 2, 3$) and $VO(OH_2)_5{\cdot}OH_2^{2+}$ could serve as test cases for new computational methods, in particular new functionals.

(iii) The Cu^+ Ion in Aqueous Solution. It is one of the few transition metal aqua ions with a 1+ charge, and its coordination number is unknown at the present time. When the geometry of $Cu(OH_2)_6^+$ is optimized in T_h symmetry with HF and SBKJ/6-31G(d) basis sets, a triply degenerate imaginary mode is obtained in the computed vibrational spectrum. At the HF level, this mode is real in the corresponding structure with S_6 symmetry, but at the MP2 level, imaginary a_2 and e modes are obtained. Obviously, hexacoordinated Cu^+ does not exist in the gas phase. The following calculations at the MP2 level are used to probe likely coordination numbers of Cu^+.

The computed vibrational spectrum of the $Cu(OH_2)_3{\cdot}(OH_2)_3^+$ species with C_3 symmetry, in which there are three Cu−O bonds of 2.050 Å and three H_2Os in the second coordination sphere, does not have any imaginary frequency. Tetracoordinated $Cu(OH_2)_4{\cdot}(OH_2)_2^+$ with two H_2Os in the second sphere and D_{2d}, D_2, C_2, and S_4 symmetry, respectively, have 4, 1, 0, and 2 imaginary frequencies. In the species with C_2 symmetry, there are two Cu−O bonds of 2.024 Å and two longer Cu−O bonds of 2.209 Å. It should be noted that within the system of one Cu^+ and six H_2Os, there is no tetracoordinated Cu^+ species with four equivalent Cu−O bonds. At the HF level, the dicoordinated $Cu(OH_2)_2{\cdot}(OH_2)_4^+$ ion has D_{2d} symmetry, whereas the MP2 and DFT species exhibit C_2 symmetry (Figure 5). Thus, in this case, (dynamic) electron correlation needs to be treated to obtain a correct tilt angle of the coordinated water molecules. The performance of the various computational methods on the Cu−O (d_0), O−H (d_1), and H···O (d_2) bond lengths (Figure 5 and Table 5) of this compound is analyzed in the following.

With respect to MP2, d_0 as well as d_2 are too long by >0.1 Å (Table 5) at the HF level. While the errors in the O−H (d_1) and H···O (d_2) bonds are similar to those seen for the 2+ and 3+ ions (Tables 1 and 2), the error in the Cu−O bonds is large. The striking difference to the previously discussed aqua ions is the large overestimation of the Cu−O bond lengths (d_0) at the HF level (Table 5). The other deviations follow the already discussed trends (Tables 1 and 2). Often, HF produces too long metal−ligand bond lengths of transition elements with filled subshells. In Cu^I, the 3d shell is filled, whereas in η^6-(C_6H_6)-$Ru(OH_2)_3^{2+}$ (see "(v) The 'Organometallic Aqua Ion', η^6-$(C_6H_6)Ru(OH_2)_3^{2+}$" section), it is the d_π ("t_{2g}") subshell. The BLYP and B3LYP functionals produce much better results than HF because they include electron correlation, whose treatment

TABLE 3: Selected Bond Lengths in the $VO(OH_2)_5^{2+}$ Ion

method	basis set	d(V═O), Å	d(V−O), Å (cis to V═O)[a]	d(V−O), Å (trans to V═O)
HF	SBKJ/6-31G(d)	1.518	2.101, 2.103	2.242
HF	SBKJ/6-311G(d)	1.512	2.098, 2.100	2.247
HF	SBKJu/6-31G(d)	1.515	2.098, 2.100	2.259
HF	SBKJu/6-311G(d)	1.511	2.096, 2.098	2.263
HF	SBKJu2/6-311G(d)	1.510	2.096, 2.098	2.263
CAS−SCF[b]	SBKJ/6-31G(d)	1.578	2.137, 2.137	2.265
CAS−SCF[b]	SBKJ/6-311G(d)	1.572	2.134, 2.134	2.268
CAS−SCF[b]	SBKJu/6-31G(d)	1.573	2.133, 2.133	2.276
CAS−SCF[b]	SBKJu/6-311G(d)	1.569	2.131, 2.131	2.280
MCQDPT2[b]	**SBKJ/6-31G(d)**	**1.608**	**2.107**, **2.108**	**2.221**
BLYP	SBKJ/6-31G(d)	1.588	2.113, 2.113	2.236
BLYP	SBKJ/6-311G(d)	1.586	2.113, 2.115	2.247
BLYP	SBKJu/6-31G(d)	1.586	2.109, 2.110	2.241
BLYP	SBKJu/6-311G(d)	1.585	2.110, 2.112	2.252
BLYP	SBKJu2/6-311G(d)	1.585	2.110, 2.111	2.252
B3LYP	SBKJ/6-31G(d)	1.562	2.093, 2.094	2.223
B3LYP	SBKJ/6-311G(d)	1.559	2.093, 2.095	2.231
B3LYP	SBKJu/6-31G(d)	1.561	2.090, 2.091	2.230
B3LYP	SBKJu/6-311G(d)	1.559	2.090, 2.092	2.238
B3LYP	SBKJu2/6-311G(d)	1.558	2.090, 2.092	2.238
SVWN[c]	SBKJ/6-31G(d)	1.568	2.028, 2.033	2.137
SVWN[c]	SBKJ/6-311G(d)	1.567	2.027, 2.034	2.144
SVWN[c]	SBKJu/6-31G(d)	1.568	2.026, 2.031	2.141
SVWN[c]	SBKJu/6-311G(d)	1.567	2.025, 2.031	2.147
SVWN[c]	SBKJu2/6-311G(d)	1.566	2.024, 2.030	2.147
SOP	SBKJ/6-31G(d)	1.575	2.040, 2.044	2.147
SOP	SBKJ/6-311G(d)	1.574	2.038, 2.044	2.154
SOP	SBKJu/6-31G(d)	1.575	2.037, 2.041	2.150
SOP	SBKJu/6-311G(d)	1.574	2.036, 2.042	2.157
SOP	SBKJu2/6-311G(d)	1.574	2.035, 2.041	2.157

[a] Two pairs of symmetry-equivalent bonds. [b] Active space: 2 π(V═O), σ(V═O), d_π, 2 π^*(V═O), σ^*(V═O). [c] Local density approximation.

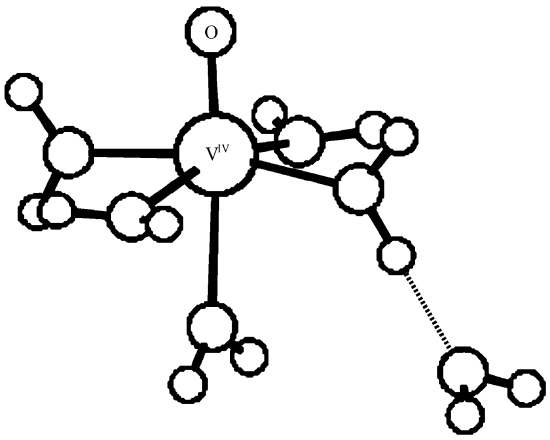

Figure 4. Perspective view of the $VO(OH_2)_5 \cdot OH_2^{3+}$ ion with C_s symmetry (CAS−SCF geometry).

is indispensable for electron-rich systems such as transition metal complexes in low oxidation states and organometallic compounds. The functionals with Slater exchange (SVWN and SOP) yield poor H···O bonds that are too short by >0.15 Å and also too short Cu−O bonds (~ 0.04−0.05 Å). Thus, such systems should be treated neither with HF nor with LDA. Good d_0, d_1, and d_2 values are obtained with the BLYP and B3LYP functionals.

(iv) Representative Transition States of Water Exchange Reactions. Representative transition states are investigated to assess the performance of the various methods on weak bonds: in the transition state for the **D** and the **A** mechanisms, respectively, there is one weak M···O bond, whereas in the interchange mechanisms, there are two weak M···O bonds (Table 6). Furthermore, the weakly bound H_2O forms H-bonds with the nearest H_2Os of the first coordination sphere. These compounds allow to verify which methods yield a balanced treatment of the M···O and the H···O bond lengths.

For sufficiently large basis sets (at least of the split-valence + polarization function quality), the M···O and H···O bond lengths are independent of its size. It should be noted that the still quite frequently used 6-311G(d) basis set[50,51] for first row transition metals produces inaccurate results because it is too small and not fully optimized. The (63311/53/41) split-valence + polarization basis set of Schäfer et al.[52] (referred to as SHA1 or SHA+ in Table 6) is better, but still too small and not as good as the SBKJ effective core potential (ECP) basis sets, in which the sp valence shells and the sp semi-cores are represented by double-ζ functions, and the valence d shell by triple-ζ functions. The latter are computationally efficient and give rise to a small BSSE (see "Basis Set Superposition Error (BSSE)" section).

In the transition state for the **D** mechanism, too long M···O and H···O bonds are obtained with HF in comparison with MP2. In contrast, DFT produces too short M···O and too long H···O bonds. This is a clear indication that the treatment of M···O and H···O bonds by DFT is not balanced correctly. In the transition states for the **A** mechanism, HF produces also too long M···O and H···O bonds in comparison with MP2. With DFT, the M···O bonds are again too short, while one of the H···O bonds is too short and the other one too long.

In the present context, the most interesting species is the transition state for the $\mathbf{I_a}$ mechanism, $[cis\text{-}V(OH_2)_5 \cdots (OH_2)_2^{2+}]^{\ddagger}$ (Figure 6), with C_2 symmetry. The corresponding trans isomer has a higher energy[33] and is not considered here. Due to the absence of static correlation, the MP2 data are most reliable. HF produces accurate V···O but too long H···O bonds. The geometry of the $[cis\text{-}V(OH_2)_5 \cdots (OH_2)_2^{2+}]^{\ddagger}$ species is not available with functionals exhibiting Becke exchange; instead, the pentacoordinated intermediate $V(OH_2)_5 \cdot (OH_2)_2^{2+}$ (Figure 7)

TABLE 4: Selected Bond Lengths in the $VO(OH_2)_5 \cdot OH_2^{2+}$ Ion

method	basis set	d(V═O), Å	d(V−O), Å (cis to V═O)	d(V−O), Å (trans to V═O)	d_0, Å	d_1, Å	d_2, Å
HF	SBKJ/6-31G(d)	1.521	2.106,[a] 2.109	2.240	2.058	0.979	1.662
HF	SBKJ/6-311G(d)	1.516	2.102,[a] 2.105	2.244	2.058	0.971	1.678
HF	SBKJu/6-31G(d)	1.518	2.102,[a] 2.106	2.256	2.055	0.979	1.662
HF	SBKJu/6-311G(d)	1.514	2.100,[a] 2.103	2.260	2.056	0.971	1.678
CAS−SCF[b]	SBKJ/6-31G(d)	1.579	2.139,[a] 2.142	2.263	2.095	0.975	1.687
CAS−SCF[b]	SBKJ/6-311G(d)	1.573	2.136,[a] 2.139	2.265	2.095	0.968	1.701
CAS−SCF[b]	SBKJu/6-31G(d)	1.574	2.135,[a] 2.139	2.274	2.092	0.975	1.686
CAS−SCF[b]	SBKJu/6-311G(d)	1.570	2.133,[a] 2.137	2.276	2.092	0.968	1.701
BLYP	SBKJ/6-31G(d)	1.590	2.118,[a] 2.128	2.245	2.056	1.049	1.509
BLYP	SBKJ/6-311G(d)	1.588	2.117,[a] 2.128	2.254	2.063	1.035	1.538
BLYP	SBKJu/6-31G(d)	1.589	2.114,[a] 2.124	2.250	2.053	1.049	1.510
BLYP	SBKJu/6-311G(d)	1.588	2.114,[a] 2.124	2.260	2.060	1.035	1.539
B3LYP	SBKJ/6-31G(d)	1.565	2.097,[a] 2.105	2.229	2.042	1.028	1.529
B3LYP	SBKJ/6-311G(d)	1.562	2.096,[a] 2.105	2.236	2.047	1.016	1.554
B3LYP	SBKJu/6-31G(d)	1.564	2.094,[a] 2.103	2.236	2.039	1.028	1.529
B3LYP	SBKJu/6-311G(d)	1.562	2.093,[a] 2.102	2.244	2.044	1.016	1.554
SVWN[c]	SBKJ/6-31G(d)	1.571	2.033,[a] 2.043	2.151	1.980	1.072	1.403
SVWN[c]	SBKJ/6-311G(d)	1.569	2.030,[a] 2.043	2.156	1.985	1.061	1.418
SVWN[c]	SBKJu/6-31G(d)	1.570	2.030,[a] 2.041	2.154	1.978	1.072	1.402
SVWN[c]	SBKJu/6-311G(d)	1.570	2.027,[a] 2.040	2.160	1.983	1.062	1.418
SOP	SBKJ/6-31G(d)	1.578	2.044,[a] 2.053	2.161	1.990	1.077	1.413
SOP	SBKJ/6-311G(d)	1.576	2.042,[a] 2.054	2.166	1.995	1.067	1.428
SOP	SBKJu/6-31G(d)	1.577	2.041,[a] 2.051	2.164	1.988	1.078	1.411
SOP	SBKJu/6-311G(d)	1.577	2.039,[a] 2.051	2.170	1.993	1.067	1.427

[a] Two symmetry-equivalent bonds. [b] Active space: 2 π(V═O), σ(V═O), d_π, 2 π^*(V═O), σ^*(V═O). [c] Local density approximation.

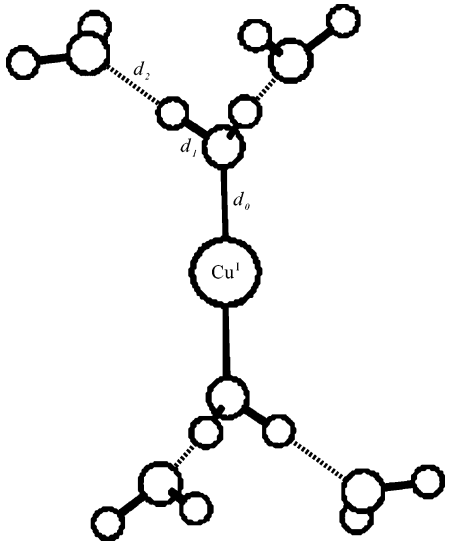

Figure 5. View along the C_2 axis of the $Cu(OH_2)_2 \cdot (OH_2)_4^+$ ion with C_2 symmetry (MP2/SBKJ/6-311G(d,p) geometry).

with two H_2Os in the second coordination sphere is obtained. Interestingly, a somewhat different [*cis*-$V(OH_2)_5 \cdots (OH_2)_2^{2+}$]‡ species (Figure 8), which is also a transition state for the water exchange reaction, is obtained on the basis of LDA (SVWN). With respect to MP2, the V···O bonds are shorter, and so are the H···O bonds. As the most noticeable difference to the MP2 and HF structures (Figure 6), the exchanging H_2Os form additional H-bonds with the equatorial H_2O ligands (italicized data in Figure 8 and Table 6), whereby a hydrogen of an exchanging H_2O forms a H-bond with the lone pair of an equatorial H_2O ligand. This type of structure (Figure 8) arises from the Slater exchange, since the SOP functional yields a similar structure. The considerably different structures obtained with ab initio MO methods (HF, MP2), and functionals with Slater (SVWN, SOP) or Becke (BLYP, B3LYP) exchange are due to the different treatment of the delicate balance between the weak V···O and H···O bonds. For functionals with Becke exchange, the H-bonds are too strong compared with the M···O bonds, whereas for functionals with Slater exchange both, the H-bonds and the M···O bonds are too strong.

TABLE 5: Selected Bond Lengths in the $Cu(OH_2)_2 \cdot (OH_2)_4^+$ Ion[a]

method	symmetry	d_0, Å	d_1, Å	d_2, Å
HF	D_{2d}	1.943, 1.953[b]	0.957, 0.954[b]	1.796, 1.822[b]
MP2	C_2	**1.830**, **1.840**,[b] **1.847**[c]	**0.984**, **0.984**, **0.983**,[b] **0.982**,[b] **0.980**,[c] **0.980**[c]	**1.695**, **1.694**, **1.672**,[b] **1.676**,[b] **1.708**,[c] **1.707**[c]
BLYP	C_2	1.858, 1.872[b]	1.007, 1.008, 1.001,[b] 1.000[b]	1.648, 1.646, 1.672,[b] 1.677[b]
B3LYP	C_2	1.855, 1.864[b]	0.992, 0.991, 0.987,[b] 0.986[b]	1.657, 1.661, 1.677,[b] 1.679[b]
SVWN[d]	C_2	1.784	1.019, 1.021	1.520, 1.519
SOP	C_2	1.791	1.026, 1.027	1.529, 1.528

[a] See Figure 5 for the meaning of d_0, d_1, and d_2. [b] 6-311G(d,p) basis set for O and H. [c] 6-311+G(d,p) basis set for O and H. [d] Local density approximation.

Starting from the LDA structure, the species with four H-bonds (Figure 8) cannot be obtained with MP2, B3LYP, and BLYP. In the transition state [*cis*-$V(OH_2)_5 \cdots (OH_2)_2^{2+}$]‡, there is a subtle balance of V···O and H···O bonds, and this species can only be obtained with appropriate methods and basis sets. Therefore, it could be used for the assessment of the performance of new functionals.

In contrast to the present B3LYP calculations, Benmelouka et al.[48] reported a [*cis*-$V(OH_2)_5 \cdots (OH_2)_2^{2+}$]‡ geometry with, however, considerably longer V···O bonds (Table 6). It is important to note that they used the rather poor 6-311G(d) basis set[50,51] (see above) for V. This is an example in which, on the basis of the combination of an inadequate computational method with a poor basis set, fortuitously, the transition state [*cis*-$V(OH_2)_5 \cdots (OH_2)_2^{2+}$]‡ could be obtained, exhibiting, however, an incorrect geometry. With B3LYP calculations based on good basis sets for V, such as SBKJ or 6-31G(d,sp) (Table 6), only the pentacoordinated intermediate $V(OH_2)_5 \cdot (OH_2)_2^{2+}$ (Figure 7) can be obtained.

(υ) The "Organometallic Aqua Ion", η^6-$(C_6H_6)Ru(OH_2)_3^{2+}$. This ion is particularly interesting because it is at the same time

TABLE 6: M···O Bond Lengths in Representative Transition States for Water Exchange Reactions via the D, I_a, and A Mechanisms

method	basis set	d(M···O), Å	d(H···O), Å[a]	ref
	(i) $[Zn(OH_2)_5\cdots OH_2^{2+}]^{\ddagger}$ (C_{2v} symmetry, **D** mechanism)			
HF	SBKJ/6-31G(d)	3.022	2.231[b]	34
HF	SBKJ/6-311G(d)	3.033	2.224[b]	this work
HF	6-31G(d,sp)[c]/6-31G(d)	2.997	2.240[b]	this work
MP2	**SBKJ/6-31G(d)**	**2.861**	**2.190**[b]	this work
MP2	**SBKJ/6-311G(d)**	**2.870**	**2.172**[b]	this work
MP2	6-31G(d,sp)[c]/6-31G(d)	2.846	2.183[b]	this work
BLYP	SBKJ/6-31G(d)	2.713	2.350[b]	this work
B3LYP	SHA1/SHA1	2.689		35
B3LYP	6-311G(d)/6-311G(d)	2.898		35
B3LYP	6-311G(d)/6-311+G(d,p)	2.829		35
B3LYP	SBKJ/6-31G(d)	2.720	2.233[b]	this work
SOP	SBKJ/6-31G(d)	2.428	2.116[b]	this work
	(ii) $[V(OH_2)_6\cdots OH_2^{3+}]^{\ddagger}$ (C_1 symmetry, **A** mechanism)			
HF	SBKJ/6-31G(d)	2.741	2.219, 2.324	this work
CAS−SCF	SBKJ/6-31G(d)	2.731	2.210, 2.345	34
MP2	SBKJ/6-31G(d)	2.692	2.150, 2.258	this work
BLYP	SBKJ/6-31G(d)	2.608	1.926, 2.752	this work
B3LYP	6-311G(d)/6-31G(d)	2.599		48
B3LYP	SBKJ/6-31G(d)	2.648	1.976, 2.540	this work
	(iii) $[Ti(OH_2)_6\cdots OH_2^{3+}]^{\ddagger}$ (C_1 symmetry, **A** mechanism)			
HF	SBKJ/6-31G(d)	2.809	2.316, 2.230	33
MP2	**SBKJ/6-31G(d)**	**2.750**	**2.257**, **2.156**	this work
BLYP	SBKJ/6-31G(d)	2.628	2.577, 2.027	this work
B3LYP	SHA+/6-311G(d)	2.686		49
B3LYP	SBKJ/6-31G(d)	2.683	2.273, 2.137	this work
	(iv) $[Sc(OH_2)_6\cdots OH_2^{3+}]^{\ddagger}$ (C_1 symmetry, **A** mechanism)			
HF	SBKJ/6-31G(d)	2.978	2.086, 2.178	34
MP2	**SBKJ/6-31G(d)**	**2.914**	**2.003**, **2.147**	this work
BLYP	SBKJ/6-31G(d)	2.768	1.967, 2.334	this work
B3LYP	SBKJ/6-31G(d)	2.797	1.953, 2.214	this work
SOP	SBKJ/6-31G(d)	2.647	1.851, 2.059	this work
	(v) [*cis*-$V(OH_2)_5\cdots(OH_2)_2^{2+}]^{\ddagger}$ (C_2 symmetry, $\mathbf{I_a}$ mechanism)			
HF	SBKJ/6-31G(d)	2.676[b]	2.271[b]	33
HF[d]	SBKJ/6-31G(d)	2.666[b]	2.286[b]	37
HF	SBKJ/6-311G(d)	2.680[b]	2.272[b]	this work
HF	6-31G(d,sp)[c]/6-31G(d)	2.672[b]	2.273[b]	this work
MP2	**SBKJ/6-31G(d)**	**2.660**[b]	**2.110**[b]	this work
MP2	6-31G(d,sp)[c]/6-31G(d)	2.594[b]	2.199[b]	this work
BLYP	SBKJ/6-31G(d)	4.083[b,f]	1.578[b,f]	this work
B3LYP	6-311G(d)/6-31G(d)	2.858[b]		48
B3LYP	6-311G(d)/6-31G(d)	2.795[b,e]	1.940[b,e]	this work
B3LYP	SBKJ/6-31G(d)	4.122[b,f]	1.586[b]	this work
B3LYP	6-31G(d,sp)[c]/6-31G(d)	4.110[b,f]	1.586[b]	this work
SOP	SBKJ/6-31G(d)	2.536[b]	1.635,[b] *1.952*[b]	this work
SVWN	SBKJ/6-31G(d)	2.517[b]	1.623,[b] *1.926*[b]	this work

[a] H-bond of the exchanging H_2O with neighboring H_2O in the first coordination sphere. [b] Two symmetry-equivalent bonds. [c] See "Basis Set Superposition Error (BSSE) section. [d] Hydration included using the self-consistent reaction field model (SCRF). [e] Recomputed using GAMESS.[21] [f] This is not the transition state for the $\mathbf{I_a}$ mechanism, but a pentacoordinated intermediate with two H-bonded H_2Os in the second sphere (see, e.g., Figure 7).

an organometallic compound and an aqua ion. In general, too long metal−carbon bonds are obtained with HF, while they are quite accurate with DFT. On the other hand, the H-bonds of aqua complexes are reproduced more accurately with HF compared to DFT. According to computations of the electron correlation using singles-doubles configuration interaction (SDCI), there might be some static electron correlation in η^6-(C_6H_6)-$Ru(OH_2)_3^{2+}$. Therefore, a "state-of-the-art" geometry optimization would require the calculation of the dynamic correlation on the basis of a multi-configuration wave function, which is prohibitive for this system. Thus, the applied methods, HF, MP2, and DFT must be considered as approximate.

Since for the present cation, no "exact" computation is feasible, and since no experimental data are available for the free ion (in the gas phase), the assessment of the accuracy of the calculations is not straightforward. This situation is encountered frequently, when chemical reactions or properties in solution are investigated. The effect of the neighbors in crystals are reproduced partially by taking into account solvation effects. Thus, geometry optimizations are performed for the hydrated η^6-$(C_6H_6)Ru(OH_2)_3^{2+}$ ion using self-consistent reaction fields (SCRF),[53−55] the polarizable continuum model (PCM),[56] and, alternatively, the cation is surrounded by six or nine quantum chemically described water molecules in the second coordination sphere (Figure 9). For the latter H_2Os, 6-31G and STO-4G[57] basis sets are used for O and H, respectively. These data are compared with that of the crystal structure of η^6-$[(C_6H_6)Ru(OH_2)_3]SO_4$ (ref 58) and serve as an indication for the adequacy of the various computational methods. In many cases, this is the only way for obtaining a clue on the accuracy of computations.

The hydrated as well as the free η^6-$(C_6H_6)Ru(OH_2)_3^{2+}$ ion exhibits C_3 symmetry. Its geometry is optimized with HF and MP2, and with DFT using the BLYP, B3LYP, SVWN (LDA),

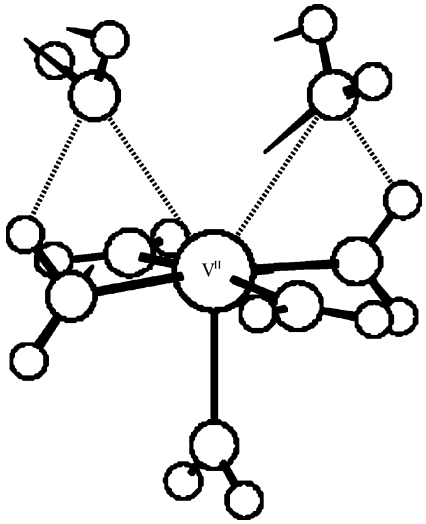

Figure 6. Perspective view and imaginary mode of the [*cis*-$V(OH_2)_5\cdots(OH_2)_2^{2+}]^{\ddagger}$ transition state with C_2 symmetry (MP2 geometry).

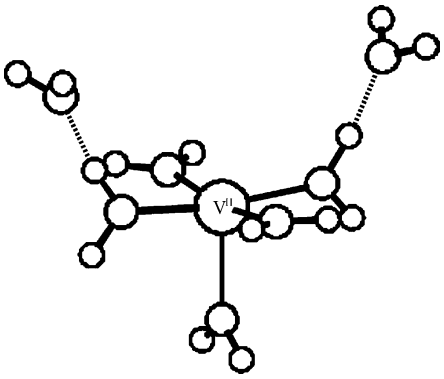

Figure 7. Perspective view of the pentacoordinated intermediate $V(OH_2)_5\cdot(OH_2)_2^{2+}$ with C_2 symmetry (B3LYP geometry).

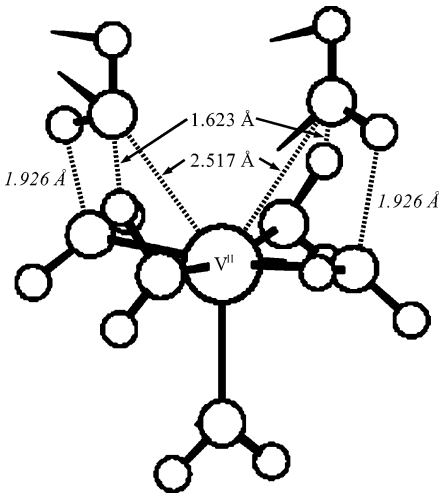

Figure 8. Perspective view and imaginary mode of the [*cis*-$V(OH_2)_5\cdots(OH_2)_2^{2+}]^{\ddagger}$ transition state with C_2 symmetry (SVWN geometry).

and SOP functionals (Table 7). For comparison, the bond lengths from the crystal structure[58] of η^6-$[(C_6H_6)Ru(OH_2)_3]SO_4$ are also included in Table 7. It should be noted that the geometry of a free ion is expected to differ from that in a crystal structure, in which there are H-bonds with the anions, for example.

Not unexpectedly, too long (by >0.3 Å) Ru−C bond lengths are obtained with HF (Table 7). They are not improved upon inclusion of hydration effects. The Ru−O bonds are slightly too long and more accurate, if hydration is included. It is

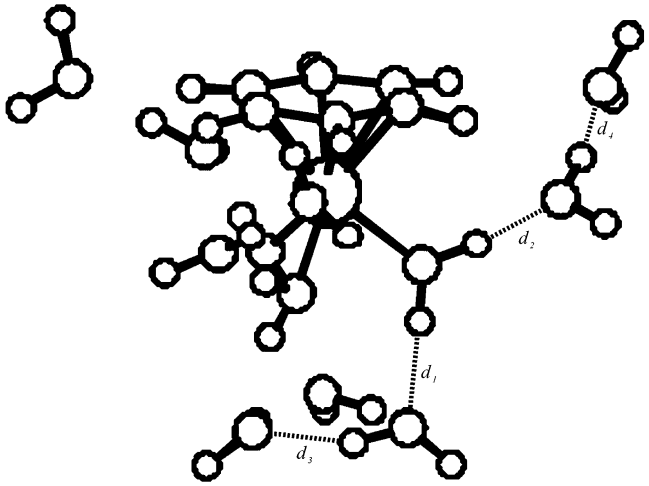

Figure 9. Perspective view of the η^6-$(C_6H_6)Ru(OH_2)_3\cdot(OH_2)_9^{2+}$ ion with C_3 symmetry (MP2 geometry).

interesting to note the differences in the Ru−C and Ru−O bonds, when the H_2O molecules in the second sphere are described quantum chemically or via effective fragment potentials (Table 7).[59,60]

Although MP2 might not be the perfectly adequate method due to the possible presence of some static electron correlation, the bond lengths of the hydrated ion agree with those in the crystal structure.

The BLYP and B3LYP functionals yield too long Ru−C and Ru−O bonds, whereby the latter are improved when hydration is included. The best results are obtained when H_2O in the second sphere is described quantum chemically. This is not unexpected, because the H-bonds between the first and the second coordination spheres are not described by the SCRF or PCM technique.

The Ru−C bond lengths, calculated with the SVWN (LDA) functional, agree with experiment, whereas the Ru−O bonds are too short (by >0.03 Å) for the ion being hydrated with explicit H_2O molecules. The most accurate (closest to the crystal structure and MP2) metal−ligand bond lengths are obtained with SVWN, when hydration is computed using the SCRF model. However, as it will be shown below, the SVWN functional is very poor for the description of H-bonds. Thus, the water exchange mechanism on η^6-$(C_6H_6)Ru(OH_2)_3^{2+}$, for example, should not be investigated using SVWN. The SOP functional yields similar, but slightly less accurate results.

It is interesting to note that the Slater exchange functional[44] produces good metal−ligand bond lengths, slightly too long C−H and O−H bonds (by >0.01 Å), but poor H-bonds (see below).

In the η^6-$(C_6H_6)Ru(OH_2)_3\cdot(OH_2)_n^{2+}$ ($n = 6$ or 9) ions (Figure 9), there are two types of H-bonds: d_1 and d_2, which are the H-bond lengths between water in the first and second coordination sphere, and d_3 and d_4, representing H-bond lengths within water molecules in the second sphere. Again, the MP2 geometries are considered the most accurate (Table 8). HF yields d_i values which are closest to MP2, but too long (by ~0.05 Å). As seen before, DFT produces too short H-bonds, whereby the largest errors are observed for LDA (SVWN functional).

It is obvious that the computation of the geometry of η^6-$(C_6H_6)Ru(OH_2)_3^{2+}$ and related ions in aqueous solution is quite demanding. LDA, producing excellent Ru−C and Ru−O bond lengths, gives rise to poor H-bonds, and therefore this method is not suitable for computations on water exchange mechanisms, for example. The Ru−O and the H-bonds are acceptable with

TABLE 7: Experimental and Calculated Bond Lengths in the η^6-$(C_6H_6)Ru(OH_2)_3^{2+}$ Ion

method	bond length, Å				
	Ru−C	Ru−O	C−C	C−H	O−H
			(i) experimental data		
X-ray diffraction[a]	2.164±0.004	2.117±0.011	1.419±0.005		
			(ii) HF		
free ion	2.456, 2.457	2.201	1.384, 1.424	1.074, 1.074	0.949, 0.948
SCRF	2.491, 2.492	2.189	1.383, 1.424	1.074, 1.074	0.950, 0.949
PCM	2.429, 2.435	2.176	1.383, 1.423	1.072, 1.073	0.949, 0.948
+ 6 H_2O[b]	2.530, 2.528	2.152	1.381, 1.422	1.073, 1.073	0.957, 0.961
+ 6 H_2O (EFP)[c]	2.480, 2.482	2.163	1.381, 1.424	1.074, 1.073	0.953, 0.953
+ 9 H_2O[b]	2.501, 2.501	2.144	1.379, 1.425	1.072, 1.074	0.955, 0.966
+ 9 H_2O (EFP)[c]	2.454, 2.455	2.161	1.381, 1.426	1.073, 1.074	0.953, 0.954
			(iii) MP2		
free ion	2.188, 2.186	2.194	1.418, 1.427	1.088, 1.088	0.973, 0.971
+ 6 H_2O[b]	2.155, 2.176	2.138	1.425, 1.422	1.087, 1.086	0.986, 0.988
+ 9 H_2O[b]	2.162, 2.161	2.130	1.419, 1.431	1.085, 1.087	0.983, 1.001
			(iv) BLYP		
free ion	2.260, 2.264	2.233	1.428, 1.440	1.093, 1.092	0.985, 0.982
SCRF	2.259, 2.258	2.219	1.425, 1.444	1.093, 1.093	0.986, 0.982
PCM	2.245, 2.242	2.197	1.423, 1.444	1.091, 1.091	0.984, 0.981
+ 6 H_2O[b]	2.242, 2.257	2.182	1.428, 1.439	1.092, 1.091	1.004, 1.009
+ 9 H_2O[b]	2.246, 2.245	2.169	1.422, 1.447	1.091, 1.092	0.999, 1.032
			(v) B3LYP		
free ion	2.256, 2.255	2.202	1.410, 1.432	1.087, 1.087	0.974, 0.971
SCRF	2.251, 2.249	2.194	1.411, 1.433	1.086, 1.086	0.974, 0.971
PCM	2.237, 2.234	2.173	1.410, 1.433	1.084, 1.085	0.973, 0.971
+ 6 H_2O[b]	2.233, 2.246	2.156	1.417, 1.426	1.086, 1.084	0.990, 0.994
+ 9 H_2O[b]	2.236, 2.235	2.145	1.409, 1.436	1.084, 1.085	0.986, 1.013
			(vi) SVWN[d]		
free ion	2.176, 2.182	2.133	1.415, 1.425	1.099, 1.098	0.989, 0.983
SCRF	2.177, 2.175	2.121	1.412, 1.429	1.098, 1.098	0.990, 0.983
+ 6 H_2O[b]	2.155, 2.178	2.086	1.420, 1.422	1.100, 1.096	1.015, 1.024
+ 9 H_2O[b]	2.161, 2.167	2.076	1.411, 1.434	1.098, 1.101	1.009, 1.058
			(vii) SOP		
free ion	2.189, 2.195	2.145	1.422, 1.432	1.105, 1.104	0.995, 0.988
SCRF	2.190, 2.187	2.132	1.419, 1.436	1.104, 1.104	0.996, 0.989

[a] X-ray crystal structure of $[\eta^6$-$(C_6H_6)Ru(OH_2)_3]SO_4$.[58] [b] Quantum chemically described H_2Os in the second coordination sphere. [c] H_2O's in the second sphere represented as effective fragment potentials.[59,60] [d] Local density approximation.

TABLE 8: H-Bond Lengths (d_1, d_2, d_3, d_4)[a] in the η^6-$(C_6H_6)Ru(OH_2)_3 \cdot (OH_2)_n^{2+}$ Ions[b]

n	d_1	d_2	d_3	d_4
		(i) HF		
6	1.828	1.752	1.804	
9	1.845	1.700	1.810	1.653
		(ii) MP2		
6	1.771	1.709	1.768	
9	1.800	1.625	1.759	1.621
		(iii) BLYP		
6	1.727	1.646	1.613	
9	1.769	1.540	1.608	1.541
		(iv) B3LYP		
6	1.727	1.653	1.641	
9	1.763	1.558	1.634	1.547
		(v) SVWN[c]		
6	1.610	1.514	1.418	
9	1.648	1.417	1.416	1.442

[a] See Figure 9. [b] Units: Å. [c] Local density approximation.

HF, but the Ru−C bonds are very inaccurate. MP2 with a quantum chemically described second coordination sphere is doubtless the best method, but prohibitive for the investigation of, for example, water exchange or substitution reactions. The MP2 geometries should be suitable for the computation of electronic spectra in aqueous solution. Since the B3LYP functional is slightly superior over BLYP, it could be an acceptable method for the geometry optimization of species participating in substitution reactions of η^6-$(C_6H_6)Ru(OH_2)_3^{2+}$, but these geometries may not be sufficiently accurate for the calculation of electronic spectra because too long metal−ligand bonds give rise to too low $d_\pi \rightarrow d_\sigma^*$ ("t_{2g}" → "e_g") transition energies. MP2 or, more preferably, CAS−SCF-based MP2 methods should be used for the computation of activation or reaction energies of such systems (whereby, of course, hydration effects have to be included).

(vi) Geometry of the $HO \cdot (H_2O)_3^-$ and $OH_3 \cdot (OH_2)_3^+$ Ions. Accurate computations on solutes in aqueous solution require techniques that describe H-bonding sufficiently well. It has been shown that for $M(OH_2)_6 \cdot OH_2^{2+}$ ions (Table 1), functionals with Slater exchange yield too short H-bonds (d_2). This error is smaller for the functionals with Becke exchange, and HF produces a similar error with an opposite sign. The geometry of $M(OH_2)_6 \cdot OH_2^{3+}$ ions, however, cannot be obtained with the currently used functionals; always the deprotonated species $MOH(OH_2)_5 \cdot H_3O^{3+}$ are obtained. For the 1+ ion, $Cu(OH_2)_2 \cdot (OH_2)_4^+$, HF produces too long Cu−O and H···O bonds (Table 5) that are, however, too short for functionals with Slater exchange. HF yields reasonable H-bonds, but very inaccurate Ru−C bonds for the η^6-$(C_6H_6)Ru(OH_2)_3^{2+}$ ion. On the other hand, LDA reproduces the Ru−C and Ru−O bonds well, but not at all the H-bonds.

To obtain additional data for the assessment of the performance of the various computational methods on H-bonding, the OH^- and the H_3O^+ ions with their most tightly bound neighbors

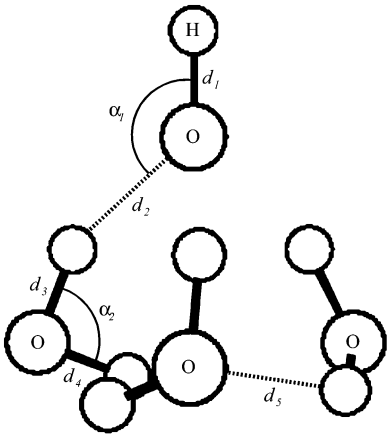

Figure 10. Perspective view of the $HO\cdot(OH_2)_3^-$ ion with C_3 symmetry (MP2 geometry).

TABLE 9: Selected Calculated Bond Lengths (d_1, d_2, d_3, d_4, d_5)[a] and Bond Angles (α_1, α_2)[a] of $HO\cdot(H_2O)_3^-$ [b]

method	d_1	d_2	d_3	d_4	d_5	α_1	α_2
HF	0.939	1.735	0.970	0.943	2.452	129.21	100.66
MP2	0.958	1.653	0.999	0.965	2.221	129.06	96.55
BLYP	0.972	1.688	1.017	0.983	2.150	129.27	96.59
B3LYP	0.961	1.679	1.003	0.970	2.171	129.53	97.52
SVWN[c]	0.968	1.593	1.027	0.997	1.848	130.18	94.77
SOP	0.974	1.604	1.032	1.003	1.864	130.07	94.69

[a] See Figure 10. [b] Units: bond lengths: Å, bond angles: °. [c] Local density approximation.

in water are investigated. The structures have been taken from snapshots of a Car−Parrinello ab initio molecular dynamics (CPMD)[61] study of OH^- or H_3O^+ in 31 H_2O molecules.[62] All of these calculations are performed using the 6-311G(d,p) basis set. The MP2 method is considered the most accurate because of the absence of static electron correlation.

The $HO\cdot(H_2O)_3^-$ ion has C_3 symmetry (Figure 10). A fourth H_2O that is bound much more weakly to OH^- (via the H of OH^-)[62] is not included in the model. The O−H bond length in hydroxide (d_1), O−H in water (d_3, d_4), the H**O···H**OH H-bond (d_2), the H_2**O···H**OH H-bond (d_5), and two bond angles (α_1, α_2) are reported in Table 9. With respect to MP2, HF yields shorter O−H bonds (d_1, d_3, d_4) and longer H···O bonds (d_2, d_5) as for the $M(OH_2)_6\cdot OH_2^{n+}$ and $MOH(OH_2)_5\cdot H_3O^{3+}$ ions (Tables 1 and 2). The B3LYP data are close to that of MP2 with a maximum deviation of −0.05 Å for d_5. The BLYP bond lengths are slightly less accurate, but BLYP produces slightly better angles than B3LYP. The worse angle (α_2) for B3LYP arises presumably from the HF portion in its exchange functional. This is evident from the least accurate α_2 angle obtained with HF. Again, the two functionals with Slater exchange, SVWN and SOP, produce the least accurate O−H and H···O bonds.

The $OH_3\cdot(OH_2)_3^+$ ion (Figure 11, Table 10) exhibits C_3 symmetry at the MP2 and DFT levels, but C_{3v} symmetry at the HF level. The deviations with respect to MP2 follow the same trends as for $HO\cdot(H_2O)_3^-$. Accurate H-bond lengths are obtained with BLYP and B3LYP, and again, the bond lengths are better with B3LYP, but the angles better with BLYP as discussed above.

For both ions, $HO\cdot(H_2O)_3^-$ and $OH_3\cdot(OH_2)_3^+$, the most accurate bond lengths with respect to MP2 are obtained with B3LYP, whereas BLYP reproduces the angles most accurately. From these data, the failure of the BLYP or B3LYP functional, in particular for the geometry of $M(OH_2)_6\cdot OH_2^{3+}$ ions and the transition state $[cis\text{-}V(OH_2)_5\cdots(OH_2)_2^{2+}]^‡$, would not have been

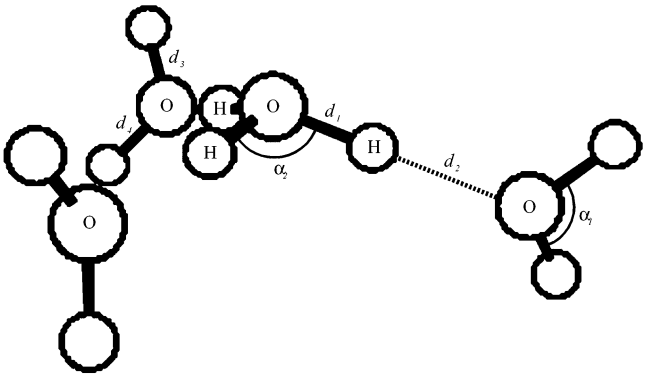

Figure 11. Perspective view of the $OH_3\cdot(H_2O)_3^+$ ion with C_3 symmetry (MP2 geometry).

TABLE 10: Selected Calculated Bond Lengths (d_1, d_2, d_3, d_4)[a] and Bond Angles (α_1, α_2)[a] of $OH_3\cdot(OH_2)_3^+$ [b]

method	d_1	d_2	d_3	d_4	α_1	α_2
HF[c]	0.980	1.608	0.944	0.944	114.96	107.64
MP2	1.008	1.536	0.962	0.962	112.51	105.72
BLYP	1.028	1.545	0.974	0.973	112.87	106.47
B3LYP	1.014	1.538	0.964	0.964	114.14	107.25
SVWN[d]	1.039	1.446	0.973	0.973	115.33	107.95
SOP	1.044	1.458	0.978	0.978	114.81	107.63

[a] See Figure 11. [b] Units: bond lengths: Å, bond angles: °. [c] C_{3v} symmetry. [d] Local density approximation.

predicted. This example shows that the adequacy of a computational method should, whenever possible, be assessed on the basis of the system of interest itself; its validation on a similar system might not be appropriate.

Energies of Aqua Ions. The relative energies of hexa- and hepta-, hexa- and penta-, and hexa- and tetracoordinated metal aqua ions are computed with ab initio MO methods and DFT. For MP2 to be appropriate, systems are chosen in which static electron correlation is absent. All of the geometry optimizations are performed for the free ions (in the gas phase) using SBKJ basis sets for the transition metals and 6-31G(d) basis sets for O and H. Some of the energies are also computed with larger basis sets for O and H. Truhlar and co-workers[63] found that for the computation of activation energies and relative energies of conformers of organic compounds, the addition of diffuse functions to split valence basis sets leads to better results at the DFT level, in particular for the modified Perdew−Wang functional, than the augmentation of the basis to a triple-ζ valence quality. Although inorganic compounds are analyzed in the present study, $\Delta E^‡$ and ΔE (see below) are also evaluated with 6-31+G(d,p) and 6-31++G(d,p) basis sets (for O and H) at the 6-31G(d) geometry, and with 6-311+G(d,p) basis sets at the 6-311G(d,p) geometry (Table 11).

The water exchange reaction on $Sc(OH_2)_6^{3+}$, which has been investigated previously[34] using HF, proceeds via the **A** mechanism (eqs 1 and 2). Since the purpose of the present calculations is to compare the total energies based on various methods, no solvation, no zero point energy, and no thermal corrections are included in the activation energy ($\Delta E^‡$) and the relative energy (ΔE) of the heptacoordinated intermediate $Sc(OH_2)_7^{3+}$ (with respect to the reactant $Sc(OH_2)_6\cdot OH_2^{3+}$).

$$Sc(OH_2)_6\cdot OH_2^{3+} \rightarrow [Sc(OH_2)_6\cdots OH_2^{3+}]^‡ \quad (1)$$

$$[Sc(OH_2)_6\cdots OH_2^{3+}]^‡ \rightarrow Sc(OH_2)_7^{3+} \quad (2)$$

For the reactant, the transition state and the heptacoordinated

TABLE 11: Activation Energies ($\Delta E^{\ddagger}$) and Relative Energies (ΔE) of Intermediates for the Water Exchange Reactions on $Sc(OH_2)_6^{3+}$ and $Zn(OH_2)_6^{2+}$ [a]

	HF geometry		MP2 geometry		BLYP geometry		SOP geometry	
method	$\Delta E^{\ddagger}$	ΔE	$\Delta E^{\ddagger}$	ΔE	$\Delta E^{\ddagger}$	ΔE	$\Delta E^{\ddagger}$	ΔE
			(i) $Sc(OH_2)_6^{3+}$ (**A** mechanism)					
HF	**22.3**, **14.3**,[d] **13.4**[e]	**0.5**, **−4.7**,[d] **−7.6**[e]	20.2	−2.1	7.7	−17.7	23.3	−9.7
MP2	27.7	7.1	**29.2**, **32.2**,[b] **32.4**,[c] **31.9**[d]	**8.9**, **11.4**,[b] **10.8**,[c] **10.7**[d]	27.1	4.1	35.7	8.2
BLYP	39.4	28.8	44.7	35.7	**52.6**, **58.9**,[b] **58.9**,[c] **56.8**[d]	**41.0**, **46.9**,[b] **46.6**,[c] **44.7**[d]	56.8	43.7
B3LYP	35.0	19.6	38.9	24.9	42.6, 47.7,[d] 45.6[e]	26.7, 31.6,[d] 28.7[e]	47.8	29.1
SOP	35.3	14.8	41.6	24.9	47.4	32.7	**43.3**	**29.6**
SVWN	35.2	13.7	41.4	23.8	46.9	31.6	42.1	27.9
			(ii) $Zn(OH_2)_6^{2+}$ (**D** mechanism)					
HF	**27.3**, **27.8**,[d] **26.9**[e]	**18.9**, **23.1**,[d] **20.8**[e]	41.0	34.2	26.9	29.8	29.4	40.0
MP2	24.7	10.7	**24.3**, **26.8**,[b] **27.3**,[c] **31.5**,[d] **29.9**[e]	**8.8**, **16.0**,[b] **15.9**,[c] **15.9**,[d] **9.7**[e]	23.6	11.5	24.8	17.0
BLYP	11.3	−9.3	10.8	−14.7	**12.9**, **16.8**,[b] **17.2**,[c] **16.3**,[d] **14.8**[e]	**−16.1**, **−2.2**,[b] **−2.0**,[c] **−2.1**,[d] **−7.6**[e]	14.0	−16.5
B3LYP	15.8	−3.1	15.3	−7.3	17.0, 19.6,[d] 18.3[e]	−6.6, 5.7,[d] 0.8[e]	17.5	−5.0
SOP	14.0	−13.7	11.1	−23.1	14.5	−28.6	**9.4**	**−31.7**
SVWN	15.2	−13.0	12.2	−22.5	15.7	−27.7	10.1	−30.7

[a] Units: kJ/mol. [b] The energy was computed with the 6-31+G(d,p) basis set. [c] The energy was computed with the 6-31++G(d,p) basis set. [d] The energy was computed with the 6-311+G(d,p) basis set. [e] The energy was computed with the 6-311G(d,p) basis set.

intermediate (eqs 1 and 2), the geometry is optimized with HF, MP2, BLYP, and SOP. For each of those four sets of geometries, $\Delta E^{\ddagger}$ and ΔE are computed with the methods used for the geometry optimizations and furthermore, with the B3LYP and SVWN functionals (Table 11).

For MP2, taken as the most accurate method (because static electron correlation is absent in these compounds), $\Delta E^{\ddagger}$ and ΔE do not depend on the size of the basis set (Table 11). These energies are also quite insensitive to the geometries since, for example, the MP2 energies at the HF, BLYP, and SOP geometries are similar. ΔE is positive, indicating that the heptacoordinated species is less stable than the hexacoordinated one. ΔE calculated with HF is almost zero and depends on the basis set: when the latter is increased, $\Delta E^{\ddagger}$ and ΔE are smaller, whereby ΔE is negative, showing that heptacoordination would be favored over hexacoordination. Obviously, HF favors the species with the higher coordination number by ∼15 kJ/mol, and $\Delta E^{\ddagger}$ follows the same trend. Because of the similarities of the BLYP and B3LYP geometries on one hand, and those of SVWN and SOP on the other hand, the geometry optimizations are performed for BLYP and SOP only. With BLYP, ΔE is also quite insensitive to the size of the basis set. However, ΔE is much larger than at the MP2 level (by ∼35 kJ/mol), and $\Delta E^{\ddagger}$ follows the same trend. The deviation with respect to MP2 is smaller for B3LYP (by ∼20 kJ/mol). Also, these data are quite independent of the size of the basis set. Clearly, the B3LYP and BLYP functionals favor the lower coordination number, whereby this bias is opposite to that of HF and considerably larger. Interestingly, the SOP and SVWN results are not worse than those of B3LYP and are even better than those of BLYP.

The water exchange mechanism on $Zn(OH_2)_6^{2+}$ (eqs 3 and 4) proceeds via the **D** (or perhaps the $\mathbf{I}_d$) mechanism. It has been investigated using HF and DFT (B3LYP).[34,35]

$$Zn(OH_2)_6^{2+} \rightarrow [Zn(OH_2)_5 \cdots OH_2^{2+}]^{\ddagger} \quad (3)$$

$$[Zn(OH_2)_5 \cdots OH_2^{2+}]^{\ddagger} \rightarrow Zn(OH_2)_5 \cdot OH_2^{2+} \quad (4)$$

At the MP2 level ΔE is positive, indicating that hexacoordination is favored over pentacoordination. ΔE increases marginally when the 6-31G(d) basis set for O and H is increased to 6-311G(d,p) (Table 11). The addition of anion diffuse functions on either basis set gives rise to a larger ΔE. For the augmented basis sets, $\Delta E^{\ddagger}$ increases similarly, whereby the 6-311G(d,p) basis does not yield a smaller value as for ΔE. At the HF level, ΔE is too large by ∼10 kJ/mol, favoring again the species with the higher coordination number. In contrast, ΔE is negative for the BLYP functional that favors the lower coordination number as for Sc^{III}. With B3LYP and the 6-31G(d) basis set, ΔE is also negative, but slightly positive with larger basis sets. The functionals with Slater exchange favor also the lower coordination number.

Whether the associative or the dissociative mechanism is investigated, the errors with respect to MP2 are the same: HF favors the *higher* coordination number by 10−15 kJ/mol, whereas DFT favors the *lower* coordination number by 15−35 kJ/mol. Correspondingly, for the **A** mechanism, $\Delta E^{\ddagger}$ is underestimated by HF, but overestimated by DFT, whereas the errors are opposite for the **D** mechanism. It should be noted that HF favors the associative pathway and DFT favors the dissociative one. This has consequences in cases in which associative and dissociative mechanisms exhibit close activation energies.

The relative energy (ΔE) of tetracoordinated $M(OH_2)_4 \cdot (OH_2)_2^{n+}$ (Figure 12) with respect to hexacoordinated $M(OH_2)_6^{n+}$ (eq 5) is calculated in order to corroborate the previous findings. Thus, if ΔE is positive, hexacoordination is favored. In the four selected metal ions with an empty, a half-filled or a filled 3d shell, there is no ligand field stabilization energy (LFSE), which could be responsible for the preference for the coordination number of 6. Static electron correlation is absent in all of these transition metal ions (Table 12). Therefore, MP2 is considered the most reliable method. The geometries are optimized with HF, MP2, BLYP, B3LYP, SVWN, and SOP using SBKJ basis sets for the transition metals and 6-31G(d) basis sets for O and H. For all of the methods except the functionals with Slater exchange, the geometry optimizations are also performed with the 6-311G(d,p) basis set for O and H, and the energies at these geometries are evaluated using the 6-311+G(d,p) basis set as well (Table 12).

$$M(OH_2)_6^{n+} \rightarrow M(OH_2)_4 \cdot (OH_2)_2^{n+} \quad (5)$$

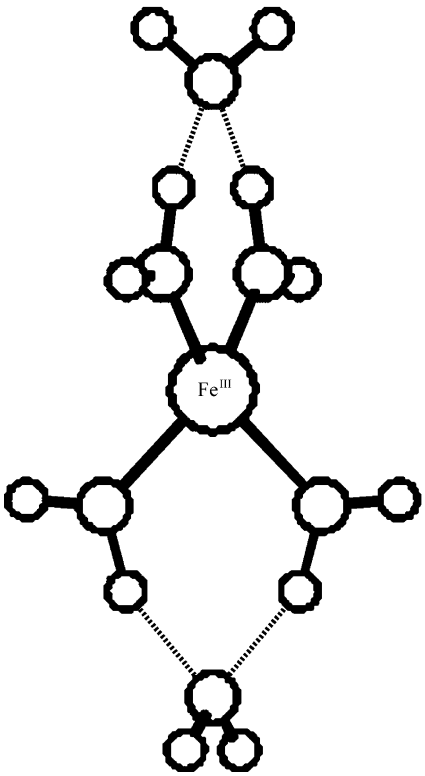

Figure 12. Perspective view of the $Fe(OH_2)_4{\cdot}(OH_2)_2^{3+}$ ion with D_{2d} symmetry (MP2/SBKJ/6-311G(d,p) geometry).

For the $M(OH_2)_4{\cdot}(OH_2)_2^{3+}$ ions (M = Sc^{III} and Fe^{III}) with a 3+ charge, the "deprotonation artifact" is not observed. As for the above-discussed aqua ions, HF overestimates slightly the M−O bond lengths and underestimates the O−H and H···O bond lengths. At the BLYP level, the Fe−O bonds are unusually inaccurate, too long by ∼0.04 Å. Otherwise, the BLYP and the B3LYP geometries are close to those of MP2, and the functionals with Slater exchange produce too short M−O and H···O bond lengths, but too long O−H bonds.

With MP2, the d^0 aqua ion of Sc^{III} is hexacoordinated due its large and positive ΔE. At the HF level, ΔE is even larger by 20−30 kJ/mol, favoring again the higher coordination number. For BLYP, ΔE is smaller (than MP2) and favors the lower coordination number by ∼55−75 kJ/mol. This error is smaller for the B3LYP functional (∼35−55 kJ/mol), but huge for the functionals with Slater exchange.

The aqua ions of Mn^{II} and Fe^{III} both have a high-spin d^5 electron configuration. The error of the various methods with respect to MP2 is similar to that of Sc^{III}. The molecular orbital methods HF and MP2 predict $Mn(OH_2)_6^{2+}$ to be more stable than $Mn(OH_2)_4{\cdot}(OH_2)_2^{2+}$, whereas BLYP predicts the opposite. According to the B3LYP calculations with the larger basis set, the hexa- and tetracoordinated species are approximately equally stable. The error of ΔE based on the functionals with Slater exchange is largest. Similar trends are observed for Fe^{III}, whereby erroneously, the functionals with Slater exchange predict tetracoordination.

The d^{10} ion Zn^{II} is particularly interesting because MP2 predicts quite similar energies for $Zn(OH_2)_6^{2+}$ and $Zn(OH_2)_4{\cdot}(OH_2)_2^{2+}$. In *aqueous solution*, Zn^{II} is known[64] to be hexacoordinated, but this is not relevant in the present context. HF predicts a coordination number of 6 in contrast to DFT. Again, the functionals with Slater exchange have the largest deviation from MP2.

To check whether the trends observed for the transition metals are also followed by systems without ("chemically relevant") d orbitals, the $Ca(OH_2)_6^{2+}/Ca(OH_2)_4{\cdot}(OH_2)_2^{2+}$ pair is investigated (Table 12). The HF, BLYP, and B3LYP Ca−O bonds are virtually equal to those of MP2, but shorter for functionals exhibiting Slater exchange. The deviations in the O−H and H···O bonds are as observed before. The error in the energy is also similar to that of the transition metals: a preference of ∼20 kJ/mol for the higher coordination number is seen for HF, but the lower coordination number is favored by ∼25−35 and ∼20−30 kJ/mol for BLYP and B3LYP, respectively. The error is huge for the functionals with Slater exchange (∼80−90 kJ/mol) that, erroneously, predict the tetracoordinated species to be more stable.

The pronounced preference of the 3+ ions for hexacoordination arises from their electrophilicity. To summarize, HF favors higher coordination numbers by ∼15−35 kJ/mol, whereas BLYP and B3LYP, respectively, show a preference for the lower coordination numbers by ∼30−90 and ∼20−65 kJ/mol. The SVWN (LDA) and SOP functionals give rise to an even larger error.

Basis Set Superposition Error (BSSE). The basis set superposition error (BSSE) is the energy by which the energy of a given atom is lowered due to the basis sets of its neighbors. In the present examples, the BSSE is the energy by which the energy of a transition metal ion in an octahedral hexaaqua complex (exhibiting T_h symmetry) is lowered by its six H_2O ligands. The BSSE is computed as the difference between the energy of the metal ion with six ghost-OH_2 ligands, $M(\text{ghost-}OH_2)_6^{n+}$ (the ghost-OH_2's are at the positions the six OH_2's would have in the corresponding $M(OH_2)_6^{n+}$ complex), and that of the free metal ion, M^{n+}, whereby for both calculations, the electron configuration of the metal must be the same as in the genuine $M(OH_2)_6^{n+}$ complex. This procedure is called the "counterpoise" method,[65] which is the best technique for the determination of BSSE corrected energies. Poor geometries arising from the BSSE are more expensive to correct.[66] Whenever possible, it is preferable and easier to chose the basis sets in such a way, that the BSSE is sufficiently small to obtain the physical property of interest with the desired accuracy.

In this section are analyzed two types of basis sets for transition metals: (i) basis sets (SBKJ)[22] in which the inner shells are described by (relativistic) effective core potentials (ECPs), the s and p semicores and the s and p valence shells each by double-ζ functions, and the d shell by triple-ζ functions, and (ii) 6-31G[67] all-electron basis sets, in which all of the shells are described by contracted Gaussians.

For all of the six investigated metal ions (Sc^{III}, V^{II}, Cr^{III}, Mn^{II}, Fe^{III}, and Zn^{II}), the BSSE of the ECP basis sets (SBKJ) is smaller than for 6-31G (Table 13). These calculations are performed at the HF level. The addition of a p-polarization function on H or the improvement of the double-ζ valence basis set to triple-ζ valence quality has a small effect on the BSSE (Zn^{II}, SBKJ data). The addition of diffuse functions on O has a larger effect, which is, however, still small (<0.5 kJ/mol). For the 3+ ion Sc^{III}, the BSSE increase arising from the addition of diffuse functions on O and H is larger; it increases by ∼4.0 kJ/mol for the addition of diffuse functions (+) to 6-31G(d) on O, and by ∼3.8 kJ/mol for their addition (++) to 6-311G(d,p) on both, O and H, (Sc^{III}, SBKJ data).

The quite large BSSE of 6-31G for the 2+ ions is reduced approximately to that of SBKJ, when diffuse d and sp functions (Table 14) are added, but the BSSE remains large for the 3+ ions. For the latter, with the exception of Fe^{III}, the BSSE is

TABLE 12: Selected Bond Lengths (d) and Relative Energies (ΔE) of $M(OH_2)_4\cdot(OH_2)_2^{n+}$ with Respect to $M(OH_2)_6^{n+}$ [a]

	$M(OH_2)_6^{n+}$			$M(OH_2)_4\cdot(OH_2)_2^{n+}$				
method	symmetry	d(M−O)	d(O−H)	symmetry	d(M−O)	d(O−H)[b]	d(H···O)	ΔE
				(i) M = Sc^{III} (n = 3)				
HF	T_h	2.185	0.958	D_{2d}	2.087	0.983, 0.961	1.784	165.8
		2.188[c]	0.956[c]		2.089[c]	0.978,[c] 0.959[c]	1.804[c]	167.9[c]
MP2	T_h	2.181	0.978	D_{2d}	2.083	1.015, 0.981	1.696	**146.6**
		2.191[c]	0.974[c]		2.092[c]	1.010,[c] 0.976[c]	1.668[c]	**135.0**[c]
								131.9[d]
BLYP	T_h	2.178	0.989	D_{2d}	2.067	1.042, 0.991	1.640	72.6
		2.187[c]	0.985[c]		2.076[c]	1.033,[c] 0.987[c]	1.666[c]	78.3[c]
								74.9[d]
B3LYP	T_h	2.163	0.979	D_{2d}	2.057	1.026, 0.982	1.647	93.7
		2.170[c]	0.976[c]		2.064[c]	1.019,[c] 0.979[c]	1.666[c]	98.6[c]
								95.0[d]
SVWN	T_h	2.112	0.989	D_{2d}	2.016	1.058, 0.992	1.524	37.9
SOP	T_h	2.122	0.995	D_{2d}	2.026	1.064, 0.997	1.534	39.5
				(ii) M = Mn^{II} (n = 2)				
HF	T_h	2.241	0.949	D_{2d}	2.127	0.961, 0.949	1.897	36.4
		2.249[c]	0.947[c]		2.133[c]	0.958,[c] 0.948[c]	1.929[c]	39.4[c]
MP2	T_h	2.216	0.968	D_{2d}	2.103	0.985, 0.968	1.819	**22.7**
		2.226[c]	0.965[c]		2.113[c]	0.980,[c] 0.964[c]	1.811[c]	**23.8**[c]
								29.7[d]
BLYP	T_h	2.215	0.980	D_{2d}	2.086	1.005, 0.979	1.762	−26.0
		2.226[c]	0.976[c]		2.097[c]	0.998,[c] 0.975[c]	1.801[c]	−14.9[c]
								−8.8[d]
B3LYP	T_h	2.205	0.970	D_{2d}	2.083	0.992, 0.969	1.766	−12.4
		2.214[c]	0.967[c]		2.092[c]	0.986,[c] 0.967[c]	1.802[c]	−2.5[c]
								2.8[d]
SVWN	T_h	2.124	0.979	D_{2d}	2.016	1.015, 0.978	1.624	−61.2
SOP	T_h	2.137	0.985	D_{2d}	2.027	1.020, 0.984	1.635	−60.4
				(iii) M = Fe^{III} (n = 3)				
HF	T_h	2.060	0.958	D_{2d}	1.947	0.986, 0.963	1.766	129.9
		2.062[c]	0.956[c]		1.946[c]	0.981,[c] 0.960[c]	1.783[c]	129.1[c]
MP2	T_h	2.047	0.978	D_{2d}	1.932	1.020, 0.982	1.677	**100.1**
		2.052[c]	0.974[c]		1.935[c]	1.015,[c] 0.977[c]	1.648[c]	**92.1**[c]
								96.2[d]
BLYP	T_h	2.082	0.989	D_{2d}	1.958	1.048, 0.992	1.622	9.9
		2.091[c]	0.985[c]		1.964[c]	1.038,[c] 0.989[c]	1.645[c]	22.2[c]
								25.8[d]
B3LYP	T_h	2.052	0.979	D_{2d}	1.932	1.032, 0.983	1.627	36.9
		2.058[c]	0.976[c]		1.937[c]	1.024,[c] 0.980[c]	1.644[c]	45.9[c]
								48.9[d]
SVWN	T_h	2.008	0.990	D_{2d}	1.895	1.065, 0.993	1.509	−16.8
SOP	T_h	2.019	0.995	D_{2d}	1.905	1.070, 0.998	1.520	−17.4
				(iv) M = Zn^{II} (n = 2)				
HF	T_h	2.134	0.949	D_{2d}	2.001	0.962, 0.950	1.888	12.4
		2.141[c]	0.947[c]		2.004[c]	0.958,[c] 0.948[c]	1.922[c]	16.3[c]
MP2	T_h	2.109	0.968	D_{2d}	1.979	0.986, 0.968	1.810	**−6.9**
		2.118[c]	0.964[c]		1.986[c]	0.981,[c] 0.964[c]	1.800[c]	**−3.7**[c]
								4.9[d]
BLYP	T_h	2.132	0.979	D_{2d}	1.995	1.004, 0.978	1.759	−49.1
		2.141[c]	0.975[c]		2.003[c]	0.997,[c] 0.974[c]	1.798[c]	−34.9[c]
								−29.5[d]
B3LYP	T_h	2.115	0.969	D_{2d}	1.981	0.992, 0.969	1.762	−36.4
		2.123[c]	0.966[c]		1.988[c]	0.986,[c] 0.966[c]	1.798[c]	−24.1[c]
								−19.4[d]
SVWN	T_h	2.041	0.978	D_{2d}	1.924	1.014, 0.977	1.625	−77.9
SOP	T_h	2.051	0.984	D_{2d}	1.933	1.019, 0.982	1.636	−77.9
				(v) M = Ca^{II} (n = 2)				
HF	T_h	2.311	0.949	D_{2d}	2.243	0.960, 0.949	1.915	70.0
		2.310[e]	0.949[e]		2.230[e]	0.960,[e] 0.949[e]	1.906[e]	65.2[e]
MP2	T_h	2.317	0.967	D_{2d}	2.247	0.982, 0.967	1.848	**49.9**
		2.311[e]	0.968[e]		2.234[e]	0.983,[e] 0.967[e]	1.836[e]	**53.5**[e]
BLYP	T_h	2.325	0.979	D_{2d}	2.248	1.001, 0.978	1.799	23.6
		2.325[e]	0.980[e]		2.233[e]	1.002,[e] 0.979[e]	1.787[e]	18.8[e]
B3LYP	T_h	2.314	0.970	D_{2d}	2.243	0.989, 0.969	1.796	30.0
		2.314[e]	0.970[e]		2.228[e]	0.990,[e] 0.969[e]	1.786[e]	25.1[e]
SVWN	T_h	2.288	0.978	D_{2d}	2.236	1.008, 0.977	1.652	−33.7
		2.285[e]	0.979[e]		2.219[e]	1.010,[e] 0.977[e]	1.644[e]	−37.2[e]
SOP	T_h	2.296	0.983	D_{2d}	2.242	1.014, 0.982	1.665	−30.5
		2.294[e]	0.984[e]		2.226[e]	1.015,[e] 0.983[e]	1.656[e]	−33.8[e]

[a] Units: bond lengths in Å and energies in kJ/mol. [b] Coordinated H_2O. [c] 6-311G(d,p) basis set for O and H. [d] The geometry was computed with the 6-311G(d,p) basis set and the energy with 6-311+G(d,p). [e] The ECP basis set of Wadt and Hay for Ca was supplemented with a d polarization function (α_d = 0.15).

TABLE 13: BSSE, Calculated for M(ghost-OH_2)$_6^{n+}$

M	electron config.	basis functions: M	basis functions: O, H	E_{tot}, hartrees	BSSE kJ/mol
Sc^{III}	d^0	SBKJ		−44.508498	ref
		SBKJ	6-31G(d)	−44.509042	−1.43
		SBKJ	6-31G+(d)	−44.510556	−5.40
		SBKJ	6-311G(d,p)	−44.509167	−1.77
		SBKJ	6-311++G(d,p)	−44.510635	−5.61
		6-31G		−758.147903	ref
		6-31G	6-31G(d)	−758.150189	−6.00
		6-31G	6-31G+(d)	−758.156731	−23.18
		6-31G	6-311G(d,p)	−758.151069	−8.31
		6-31G	6-311++G(d,p)	−758.157520	−25.25
		6-31G(d,sp)		−758.149039	ref
		6-31G(d,sp)	6-31G(d)	−758.150923	−4.95
		6-31G(d,sp)	6-311++G(d,p)	−758.157670	−22.66
		6-31G(d,sp)[a]		−758.160910	ref
		6-31G(d,sp)[a]	6-31G(d)	−758.160920	−0.03
		6-31G(d,sp)[a]	6-311++G(d,p)	−758.161011	−0.27
V^{II}	d^3 (t_{2g}^3 e_g^0)	SBKJ		−69.983752	ref
		SBKJ	6-31G(d)	−69.984170	−1.10
		SBKJ	6-311++G(d,p)	−69.984568	−2.14
		6-31G		−942.084415	ref
		6-31G	6-31G(d)	−942.085549	−2.98
		6-31G	6-311++G(d,p)	−942.086323	−5.01
		6-31G(d,sp)		−942.085717	ref
		6-31G(d,sp)	6-31G(d)	−942.085974	−0.67
		6-31G(d,sp)	6-311++G(d,p)	−942.086357	−1.68
		6-31G(d,sp)[a]		−942.085981	ref
		6-31G(d,sp)[a]	6-31G(d)	−942.086214	−0.61
		6-31G(d,sp)[a]	6-311++G(d,p)	−942.086435	−1.19
Cr^{III}	d^3 (t_{2g}^3 e_g^0)	SBKJ		−84.024815	ref
		SBKJ	6-31G(d)	−84.025194	−1.00
		SBKJ	6-311++G(d,p)	−84.025463	−1.70
		6-31G		−1041.355437	ref
		6-31G	6-31G(d)	−1041.357779	−6.15
		6-31G	6-311++G(d,p)	−1041.362852	−19.47
		6-31G(d,sp)		−1041.356288	ref
		6-31G(d,sp)	6-31G(d)	−1041.358516	−5.85
		6-31G(d,sp)	6-311++G(d,p)	−1041.363502	−18.94
		6-31G(d,sp)[a]		−1041.365521	ref
		6-31G(d,sp)[a]	6-31G(d)	−1041.365976	−1.19
		6-31G(d,sp)[a]	6-311++G(d,p)	−1041.366659	−2.99
Mn^{II}	d^5 (t_{2g}^3 e_g^2)	SBKJ		−102.424837	ref
		SBKJ	6-31G(d)	−102.425244	−1.07
		SBKJ	6-311++G(d,p)	−102.425667	−2.18
		6-31G		−1148.967760	ref
		6-31G	6-31G(d)	−1148.971800	−10.61
		6-31G	6-311++G(d,p)	−1148.973084	−13.98
		6-31G(d,sp)		−1148.972417	ref
		6-31G(d,sp)	6-31G(d)	−1148.972981	−1.48
		6-31G(d,sp)	6-311++G(d,p)	−1148.973388	−2.55
		6-31G(d,sp)[a]		−1148.972784	ref
		6-31G(d,sp)[a]	6-31G(d)	−1148.973254	−1.23
		6-31G(d,sp)[a]	6-311++G(d,p)	−1148.973610	−2.17
Fe^{III}	d^5 (t_{2g}^3 e_g^2)	SBKJ		−120.688774	ref
		SBKJ	6-31G(d)	−120.689220	−1.17
		SBKJ	6-311++G(d,p)	−120.689595	−2.16
		6-31G		−1260.442090	ref
		6-31G	6-31G(d)	−1260.445428	−8.76
		6-31G	6-311++G(d,p)	−1260.447441	−14.05
		6-31G(d,sp)		−1260.442749	ref
		6-31G(d,sp)	6-31G(d)	−1260.446154	−8.94
		6-31G(d,sp)	6-311++G(d,p)	−1260.448387	−14.80
		6-31G(d,sp)[a]		−1260.447456	ref
		6-31G(d,sp)[a]	6-31G(d)	−1260.448868	−3.71
		6-31G(d,sp)[a]	6-311++G(d,p)	−1260.449766	−6.06
		6-31G(d,sp)[b]		−1260.449489	ref
		6-31G(d,sp)[b]	6-31G(d)	−1260.450898	−3.70
		6-31G(d,sp)[b]	6-311++G(d,p)	−1260.451778	−6.01
		6-31G[c]		−1260.448865	ref
		6-31G[c]	6-31G(d)	−1260.449879	−2.66
		6-31G[c]	6-311++G(d,p)	−1260.450277	−3.71
Zn^{II}	d^{10} (t_{2g}^6 e_g^4)	SBKJ		−224.049331	ref
		SBKJ	6-31G(d)	−224.049510	−0.47
		SBKJ	6-31G(d,p)	−224.049536	−0.54
		SBKJ	6-311G(d)	−224.049542	−0.55
		SBKJ	6-311G(d,p)	−224.049572	−0.63
		SBKJ	6-31+G(d)	−224.049687	−0.93
		SBKJ	6-31G++(d,p)	−224.049756	−1.12
		SBKJ	6-311+G(d)	−224.049706	−0.98
		SBKJ	6-311++G(d,p)	−224.049759	−1.12
		6-31G		−1776.612074	ref
		6-31G	6-31G(d)	−1776.629541	−45.86
		6-31G	6-311++G(d,p)	−1776.633893	−57.29
		6-31G(d,sp)		−1776.638667	ref
		6-31G(d,sp)	6-31G(d)	−1776.639960	−3.39
		6-31G(d,sp)	6-311++G(d,p)	−1776.640467	−4.73
		6-31G(d,sp)[a]		−1776.640431	ref
		6-31G(d,sp)[a]	6-31G(d)	−1776.641545	−2.92
		6-31G(d,sp)[a]	6-311++G(d,p)	−1776.641874	−3.79

[a] The outermost of the 3s/3p functions are uncontracted. [b] The outermost of the 2s/2p and the 3s/3p functions are uncontracted. [c] The outermost of the 3s/3p and 3d functions are uncontracted.

TABLE 14: Exponents of the Diffuse d and sp Functions Added to the 6-31G Basis Set[a]

M	α(d)	α(sp)
Sc	0.0598	0.0115
V	0.0953	0.0129
Cr	0.111	0.0135
Mn	0.128	0.0140
Fe	0.138	0.0148
Zn	0.195	0.0170

[a] The diffuse functions were calculated as described by Giordan and Custodio.[28]

reduced by uncontracting the semicores to double-ζ. The added (diffuse) d and sp functions do not lower the BSSE of the 3+ ions (Fe^{III} data). The BSSE of Fe^{III} is not lowered significantly by uncontracting the 3s/3p and the 2s/2p shells, but uncontracting the 3d shell together with the 3s/3p shells reduces the BSSE which, however, remains appreciable. For Fe^{III}, either some exponents should be reoptimized or another basis set should be chosen.

For too small or not sufficiently flexible basis sets such as, for example, the unmodified 6-31G basis sets for transition metals, the BSSE increases strongly upon the addition of diffuse functions on the ligand atoms. For Sc^{III}, the augmentation of the 6-31G(d) and 6-311G(d,p) basis sets of the "ghost" water ligands with diffuse functions gives rise to the considerable BSSE increase of ∼17.2 and ∼16.9 kJ/mol, respectively. It should be noted that the BSSE increase for the improvement of 6-31G(d) to 6-311G(d,p) is much smaller (∼2.3 kJ/mol). This illustrates that diffuse functions have to be used with care by ensuring that the neighboring atoms exhibit sufficiently good basis sets. In case of doubt, the BSSE should be calculated for representative compounds and, if necessary, the basis set should be modified or chosen in such a way that the BSSE is sufficiently small.

Discussion

In this section, consequences of inappropriate basis sets and computational methods are discussed on the basis of examples involving aqua ions. In the first section are shown in a general way the consequences of inadequate basis sets. In the second and third sections, conclusions derived from inaccurate geometries and energies of aqua ions are analyzed. As examples are chosen quantum chemical calculations on water exchange reactions and the coordination number of some metal aqua ions, for which the coordination number is not known unambiguously on the basis of experimental data. This is a fundamental aspect of the chemistry of aqua ions and a prerequisite for the elucidation of their water exchange, substitution, and electron-transfer mechanisms.

Basis Sets. More often than assumed, results of quantum chemical calculations are affected by inappropriate basis sets. Still, basis sets for transition metals that are too small or not sufficiently flexible, such as 3-21G,[68] 6-311G(d),[50,51] or (63311/53/41),[52] for example, are used. Since they are too small or not sufficiently flexible, their deficiencies are usually not remedied by the addition of basis functions on the metal and the ligands. On the contrary, as shown in the "Basis Set Superposition Error (BSSE)" section, the addition of diffuse functions on ligand atoms might cause a strong increase of the BSSE, which is responsible for the drop of accuracy with improvement of the basis set. This behavior manifests itself in total energies or energy differences (e.g., reaction energies, activation energies) or bond lengths or angles getting worse upon the augmentation of basis sets, whereby the effect may be blatant, when diffuse functions are added. It should be noted, however, that it is not always inadequate basis sets for the metal that are responsible for inaccurate results. Too small basis sets on ligand atoms may also be at the origin of poor energies, geometries, or vibrational frequencies. To get reliable results for compounds with first and second row elements, basis sets of at least a split-valence + polarization quality should be used. In some cases, the omission of polarization functions on first row elements does not deteriorate the result, but the consequences of their inappropriate omission on (first row) elements in anions or systems with π bonds can be seen in inaccurate properties. Second row elements, especially those in the right block of the periodic table, should always be supplemented with polarization functions.

Geometries. Hartmann et al. studied[49] the water exchange mechanism on $Ti(OH_2)_6^{3+}$ on the basis of the bridging structure of $Ti(OH_2)_6{\cdot}OH_2^{3+}$, in which no "spontaneous" proton transfer occurred. They, however, noted that the computation of the transition state and the pentacoordinated intermediate for the **D** mechanism was not possible due to deprotonation. In fact, this was also observed in the HF/CAS−SCF studies[33,34] on the **D** mechanism for Sc^{III}, Ti^{III}, V^{III}, and Fe^{III}. This is the reason, why for these ions, a lower limit for the activation energy had to be estimated on the basis of the pentacoordinated intermediates $M(OH_2)_5{\cdot}(OH_2)_2^{3+}$ (M = Sc^{III}, Ti^{III}, V^{III}, and Fe^{III}), in which the deprotonation did not take place. The "spontaneous" deprotonation prompted Hartmann et al.[49] to investigate the H^+ transfer in the bridging $Ti(OH_2)_6{\cdot}OH_2^{3+}$ species. They found a very low activation barrier (5.4 kJ/mol) without zero point energy (ZPE) corrections and an activationless H^+ transfer when the ZPE was included. For this kind of reactions, hydration effects must be included. The present data indicate that DFT is inappropriate for aqua complexes, especially those with a 3+ charge, because it does not reproduce H-bonding correctly.

The geometries of aqua ions with a 3+ charge are quite sensitive to the computational method (Tables 1 and 2), and so are also the energies (Table 11). Thus, apart from the necessity to treat solvation, quantum chemical calculations at an appropriate level are required for both the geometry optimizations as well as the energy computations (that do not need to be performed with the same technique). Possibly, for better models involving, for example, a quantum chemically described second coordination sphere, the results might be less sensitive to the computational methods.

In a reinvestigation[48] of the water exchange mechanisms on $V(OH_2)_6^{2+}$ and $V(OH_2)_6^{3+}$ using the B3LYP functional, the deprotonation artifact was also observed for $V(OH_2)_6{\cdot}OH_2^{3+}$ with a singly bound water in the second sphere. Clearly, such spontaneous "deprotonations" are due to limitations of DFT. These observations are in line with the known inadequacy of the widely used functionals, such as LDA, BLYP, and B3LYP, for the description of H^+ transfer reactions.[69,70] In the same article, the water exchange reaction on $V(OH_2)_6^{2+}$ was claimed[48] to follow the **I** mechanism. This conclusion is at variance with experiment[71] and previous calculations[33,37] as well, which both argue in favor of the $\mathbf{I}_a$ mechanism. In the previous section, it has been shown that this incorrect conclusion is due to an incorrect geometry for the transition state arising from an inadequate computational method and basis set for V.

Energies. In contrast to earlier experimental studies,[72,73] in which experimental evidence for a coordination number of 7 for the aqua ion of Sc^{III} was presented, a more recent combined Raman and ab initio MO study[74] supplied evidence for a coordination number of 6. In a study of the water exchange mechanism on $Sc(OH_2)_6^{3+}$ on the basis of a gas-phase model,[34] the small energy difference of ~0.5 kJ/mol between the hexa- and the heptacoordinated species, obtained at the HF level, lead to the suggestion that $Sc(OH_2)_7^{3+}$ might coexist with $Sc(OH_2)_6^{3+}$ in aqueous solution. The present data show that this suggestion is wrong, and that it is due to an artifact of the HF method which overestimates the stability of the species with a higher coordination number.

In an experimental and theoretical gas phase study on $Mn(OH_2)_n^{2+}$ and $Mn(CH_3OH)_n^{2+}$ clusters by Cox et al.,[75] the tetracoordinatated $Mn(OH_2)_4{\cdot}(OH_2)_2^{2+}$ species (with the same structure as in Figure 12) was found to be more stable by 24 kJ/mol than hexacoordinated $Mn(OH_2)_6^{2+}$. The computations were performed with DFT, whereby triple-ζ + polarization and double-ζ + polarization basis sets have been used for Mn and C, O, H, respectively. The Becke-Perdew (BP) functional[38,76] used by Cox et al. is similar to BLYP, their basis sets similar to SBKJ/6-31G(d) and indeed, their result is close to the 26 kJ/mol in favor of $Mn(OH_2)_4{\cdot}(OH_2)_2^{2+}$ found in the present BLYP calculation (Table 12). At the more accurate and more reliable MP2 level, however, $Mn(OH_2)_6^{2+}$ is predicted to be more stable (Table 12). Thus, the assertion that $Mn(OH_2)_4{\cdot}(OH_2)_2^{2+}$ is more stable than $Mn(OH_2)_6^{2+}$ is most likely incorrect.

The claim by Pasquarello et al.,[77] that the Cu^{2+} ion in aqueous solution might be pentacoordinated, has shaken the established belief in the Jahn−Teller distorted $Cu(OH_2)_6^{2+}$ ion. This statement was based on a combined neutron diffraction and CPMD[61] study. The results from the second difference isotopic substitution method in neutron diffraction have been questioned in a subsequent EXAFS study,[78] in which evidence for the existence of the $Cu(OH_2)_6^{2+}$ with four Cu−O bonds of 1.95±0.01 Å and two Cu−O bonds of 2.29±0.03 Å was presented. Water in the second coordination sphere was found at a mean Cu···O distance of 4.17 Å. About at the same time, Cu^{2+} was reported[79] to be pentacoordinated with four short

(1.956±0.004 Å) and a single long (2.36±0.02 Å) Cu−O bond on the basis of a combined EXAFS and XANES study. The computations of Pasquarello et al.[77] were performed using the BLYP functional which, according to the present study, favors in all of the investigated examples the lower coordination number by more than 15 kJ/mol. Therefore, their CPMD simulations might be biased toward the lower coordination number and cannot be taken as safe evidence for the existence of pentacoordinated Cu^{2+} as the most abundant species in aqueous solution. They validated their procedure on Ni^{2+} which was calculated to be hexacoordinated. This validation is insignificant because of the large LFSE in octahedral Ni^{II} complexes, which amounts to ∼100 kJ/mol. The Mn^{2+} and the Zn^{2+} ions, with a LFSE of 0, would have been a more appropriate choice. Furthermore, the uniform background negative charge to ensure charge neutrality and the size of the simulated system, 50 water molecules and one Cu^{2+} ion in a periodically repeated box, might also give rise to (yet unknown) errors. According to the most recent CPMD study, also based on the BLYP functional, but a different basis set, the average coordination number of Cu^{2+} was found to be 5.7.[80]

Recently, Schwenk and Rode published two hybrid quantum mechanical/molecular mechanics (QM/MM) studies[81,82] on the Cu^{2+} ion in 499 H_2O molecules. In the first study,[81] in which the QM part was treated with HF, and the MM part with three-body molecular dynamics (MD), they found that Cu^{2+} is hexacoordinated with four Cu−O bonds of 2.07 Å and two Cu−O bonds of 2.2 Å. This result might be biased toward the higher coordination number because of the QM part that was treated at the HF level. In their second study,[82] the first and the second coordination spheres were included in the QM part, which was treated with HF, B3LYP, and RIDFT (resolution of the identity DFT),[83] the latter exhibiting a BP functional which is similar to BLYP (see above). For the QM part treated with HF and B3LYP, exhibiting a bias toward the higher and the lower coordination number, respectively, the Cu^{2+} ion was found to be hexacoordinated. However, an average coordination number of 5.4 was found with RIDFT. This result is in line with the present findings and proves the quite pronounced preference of BLYP (and BP) for the lower coordination number.

Taking into account the limitations of the various quantum chemical techniques, the calculations indeed supply strong evidence in favor of a Jahn−Teller distorted $Cu(OH_2)_6^{2+}$ ion in aqueous solution. Another experimental quantity, the activation volume ($\Delta V^{\ddagger}$) of 2.0±1.5 cm^3/mol (ref 84) can also be taken as a support for hexacoordination because in putative $Cu(OH_2)_5^{2+}$ the water exchange mechanism would be expected to be associative (**I_a** or **A**) which would give rise to a *negative* $\Delta V^{\ddagger}$ unless, quite unlikely, a dissociative mechanism (**I_d** or **D**) via tetracoordinated Cu^{2+} would operate.

In the 1+ ion $Cu(OH_2)_2{\cdot}(OH_2)_4^{+}$ (Figure 5), Cu−O bonds that are too long by >0.1 Å are obtained at the HF level (Table 5). In a recent QM/MM study[85] on the structure and dynamics of Ag^+ in aqueous solution, an average coordination number of 5.5 was reported, which is probably too high because HF, with which the QM part was treated, favors the higher coordination number and because the computed Ag−O bonds are most likely too long as for Cu^+. The too long Ag−O bonds give rise to a reduction of the water−water repulsion in the first coordination sphere, and this could lead to an overestimated coordination number.

The coordination number of Ca^{2+} in aqueous solution is currently investigated experimentally and theoretically. According to the most recent EXAFS and XANES study,[86] its coordination number is 7. This result was corroborated in a subsequent MD-EXAFS study that was based on a polarizable potential model.[87] QM/MM calculations,[88] in which the QM part was treated with HF and B3LYP, predicted coordination numbers of 7.6 and 8.1, respectively. Contrary to the present gas-phase calculations on $Ca(OH_2)_6^{2+}$ and $Ca(OH_2)_4{\cdot}(OH_2)_2^{2+}$ (Table 12), HF gives rise to a slightly lower mean coordination number than B3LYP. This is probably due to the MM treatment of the bulk solvent, and this example shows that the results from the gas-phase calculations have to be applied with care to the assessment of the accuracy of QM/MM computations. At variance with the QM/MM study, a coordination number of 6 was obtained in a CPMD[61] study by Bakó et al.[89] with the BLYP functional, 54 H_2O molecules in a periodic box, and a homogeneous background negative charge. A few months later, Naor et al.[90] published a coordination number between 7 and 8, based on a CPMD study similar to that of Bakó et al. with, however, only 31 H_2O molecules and a smaller basis set for Ca. Quantum chemical calculations based on cluster models, whereby hydration was treated with PCM at the MP2 level, indicate that the $Ca(OH_2)_6^{2+}/Ca(OH_2)_7^{2+}$ energy difference is <10 kJ/mol, and that of $Ca(OH_2)_7^{2+}/Ca(OH_2)_8^{2+}$ is ∼15 kJ/mol.[91] Obviously, the small energy differences between hexa-, hepta-, and octacoordinated Ca^{2+} are beyond the accuracy of the presently available models and computational methods.

The effect of the charge compensation with a uniform background charge as a replacement of anions on the results has not yet been investigated systematically and should be considered as unknown. The study of Bakó et al.[89] with a larger basis set for Ca and 54 instead of only 31 H_2O molecules appears more reliable, although the coordination number found by Naor et al.[90] agrees with experiment[86] and the QM/MM study[88] as well. In fact, an underestimated coordination number would have been expected for both CPMD studies, since they both were performed using the BLYP functional. Most likely, the QM/MM and the CPMD calculations[88−90] are not sufficiently accurate for the determination of the coordination number of Ca^{2+}.

Summary

A selection of aqua complexes covering a spectrum of demands to the computational methods and basis sets has been studied. The ab initio MO methods HF and CAS−SCF, and DFT (BLYP, B3LYP, SVWN, SOP) as well, yield an unbalanced treatment of metal−ligand and H-bond strengths. This is the reason for the preference of the higher or lower coordination number of aqua ions by HF or DFT, respectively, which is also responsible for the corresponding preference for the associative (**A/I_a**) or dissociative (**D/I_d**) substitution mechanism. In systems with weak bonds, such as transition states, disparate structures might be obtained with the various quantum chemical methods, also because of this unequal treatment of the various bond types. MP2, adequate when static electron correlation is absent, and MCQDPT2, necessary when it is present, give rise to a balanced description of the various kinds of bonds (M−L, M···L, O−H, H···O, etc.).

It is important to note that the present statements are valid for the currently used functionals BLYP, B3LYP, and LDA. Since the development of new functionals is an active research area, the situation of DFT might change in the future, whereby the presently investigated compounds could serve as a basis for the assessment of the performance of new functionals.

Limitations of HF. (i) Too long metal−ligand bond lengths might be obtained in organometallic compounds and in com-

plexes with metals in low oxidation states. (ii) A preference for the higher coordination number by typically ∼15−20 kJ/mol has to be expected, (iii) thus, HF favors the $\mathbf{I}_a$/**A** substitution mechanisms over $\mathbf{I}_d$/**D**. (iv) The metal−ligand and the hydrogen bonds are not balanced correctly.

Limitations of DFT. (i) In relatively highly charged metal complexes (3+ or higher), H-bonding might not be described correctly (viz. "spontaneous" proton transfer in $M(OH_2)_6{}^{\bullet}OH_2{}^{3+}$). (ii) LDA, and also other functionals with Slater exchange, describe H-bonding poorly. (iii) The BLYP and B3LYP functionals favor the lower coordination number by typically ∼15−75 and ∼10−55 kJ/mol, respectively; the error is considerably larger for LDA and SOP, (iv) thus, DFT favors the $\mathbf{I}_d$/**D** substitution mechanisms over $\mathbf{I}_a$/**A**. (v) These limitations are also valid for AIMD and CPMD simulations, if they are performed with the current functionals (BLYP, LDA, etc.). (vi) According to the present examples, the functionals with Becke exchange are superior over those with Slater exchange. (vii) The metal−ligand and hydrogen bond strengths are not balanced correctly, especially in complexes exhibiting a high (≥ 2+) charge.

Basis Set Limitations. (i) All-electron basis sets for transition metals and in general heavy elements, might give rise to a large BSSE, if they are too small or not adapted to the system via the addition and/or uncontraction of basis functions; the BSSE is much smaller for ECP basis sets. (ii) Too small basis sets for ligand atoms, in particular if they are anionic or if they exhibit π bonds, might lead to inaccurate or incorrect results.

Recommendations. Geometry can be computed with the most efficient method yielding the necessary accuracy, since the energy is, in the present cases (this must always be verified), not very sensitive to the geometry. For systems in solution, solvation should be included. The energy should be calculated with ab initio MO methods treating electron correlation adequately. The CAS−SCF based MP2 methods are most suitable for transition metal complexes because static and dynamic electron correlation can be treated in a straightforward manner.

Acknowledgment. One reviewer is acknowledged for his helpful comments, and special thanks to Dr. M. W. Schmidt for solving a problem with the numerical gradient in GAMESS, occurring on some machines. Dedicated to Professor Michael Grätzel on the occasion of his 60th birthday.

References and Notes

(1) Couty, M.; Hall, M. B. *J. Comput. Chem.* **1996**, *17*, 1359.
(2) Couty, M.; Bayse, C. A.: Jiménez-Cataño, R.: Hall, M. B. *J. Phys. Chem.* **1996**, *100*, 13976.
(3) Niu, S.; Hall, M. B. *J. Phys. Chem. A* **1997**, *101*, 1360.
(4) Thomas, J. L. C.; Hall, M. B. *Organometallics* **1997**, *16*, 2318.
(5) Lin, Z.; Hall, M. B. *Coord. Chem. Rev.* **1994**, *135/136*, 845.
(6) Pietsch, M. A.; Couty, M.; Hall, M. B. *J. Phys. Chem.* **1995**, *99*, 16315.
(7) Hall, M. B.; Margl, P.; Náray-Szabó, G.; Schramm, V. L.; Truhlar, D. G.; van Santen, R. A.; Warshel, A. Whitten, J. L. *ACS Symp. Ser.* **1999**, *721*, 2.
(8) Møller, C.; Plesset, M. S. *Phys. Rev.* **1934**, *46*, 618.
(9) Shavitt, I. In *Modern Theoretical Chemistry*; Schaefer, H. F., Ed.; Plenum Press: New York, 1977; Vol. 3, p 189.
(10) Raghavachari, K.; Anderson, J. B. *J. Phys. Chem.* **1996**, *100*, 12960.
(11) Roos, B. O. In *Ab Initio Methods in Quantum Chemistry II*; Lawley, K. P., Ed.; Wiley: New York, 1987.
(12) Andersson, K.; Malmqvist, P. Å.; Roos, B. O.; Sadley, A. J.; Wolinski, K. *J. Phys. Chem.* **1990**, *94*, 5483.
(13) Andersson, K.; Malmqvist, P. Å.; Roos, B. O. *J. Chem. Phys.* **1992**, *96*, 1218.
(14) Nakano, H. *J. Chem. Phys.* **1993**, *99*, 7983.
(15) Nakano, H. *Chem. Phys. Lett.* **1993**, *207*, 372.
(16) Helm, L.; Merbach, A. E. *Coord. Chem. Rev.* **1999**, *187*, 151.
(17) Erras-Hanauer, H.; Clark, T.; van Eldik, R. *Coord. Chem. Rev.* **2003**, *238−239*, 233.
(18) Curtiss, L. A.; Raghavachari, K.; Redfern, P. C.; Rassolov, V.; Pople, J. A. *J. Chem. Phys.* **1998**, *109*, 7764.
(19) *Quantum-Mechanical Prediction of Thermochemical Data*; Cioslowski, J., Ed.; Understanding Chemical Reactivity Series, Vol. 22; Kluwer: Dordrecht, 2001.
(20) Lynch, B. J.; Truhlar, D. G. *J. Phys. Chem. A* **2003**, *107*, 3898.
(21) Schmidt, M. W.; Baldridge, K. K.; Boatz, J. A.; Elbert, S. T.; Gordon, M. S.; Jensen, J. H.; Koseki, S.; Matsunaga, N.; Nguyen, K. A.; Su, S. J.; Windus, T. L.; Dupuis, M.; Montgomery, J. A. *J. Comput. Chem.* **1993**, *14*, 1347.
(22) Stevens, W. J.; Krauss, M.; Basch, H.; Jasien, P. G. *Can. J. Chem.* **1992**, *70*, 612.
(23) Hehre, W. J.; Ditchfield, R.; Pople, J. A. *J. Chem. Phys.* **1972**, *56*, 2257.
(24) Ditchfield, R.; Hehre, W. J.; Pople, J. A. *J. Chem. Phys.* **1971**, *54*, 724.
(25) Krishnan, R.; Binkley, J. S.; Seeger, R.; Pople, J. A. *J. Chem. Phys.* **1980**, *72*, 650.
(26) Schäfer, A.; Horn, H.; Ahlrichs, R. *J. Chem. Phys.* **1992**, *97*, 2571.
(27) Wadt, W. R.; Hay, P. J. *J. Chem. Phys.* **1985**, *82*, 284.
(28) Giordan, M.; Custodio, R. *J. Comput. Chem.* **1997**, *18*, 1918.
(29) Miller, W. H.; Handy, N. C.; Adams, J. E. *J. Chem. Phys.* **1980**, *72*, 99.
(30) Bender, C. F.; Davidson, E. R. *J. Phys. Chem.* **1966**, *70*, 2675.
(31) Choe, Y.-K.; Witek, H. A.; Finley, J. P.; Hirao, K. *J. Chem. Phys.* **2001**, *114*, 3913.
(32) Ivanic, J. *J. Chem. Phys.* **2003**, *119*, 9364.
(33) Rotzinger, F. P. *J. Am. Chem. Soc.* **1996**, *118*, 6760.
(34) Rotzinger, F. P. *J. Am. Chem. Soc.* **1997**, *119*, 5230.
(35) Hartmann, M.; Clark, T.; van Eldik, R. *J. Am. Chem. Soc.* **1997**, *119*, 7843.
(36) Kowall, Th.; Caravan, P.; Bourgeois, H.; Helm, L.; Rotzinger, F. P.; Merbach, A. E. *J. Am. Chem. Soc.* **1998**, *120*, 6569.
(37) Rotzinger, F. P. *Helv. Chim. Acta* **2000**, *83*, 3006.
(38) Becke, A. D. *Phys. Rev. A* **1988**, *38*, 3098.
(39) Lee, C.; Yang, W.; Parr, R. G. *Phys. Rev. B* **1988**, *37*, 785.
(40) Miehlich, B.; Savin, A.; Stoll, H.; Preuss, H. *Chem. Phys. Lett.* **1989**, *157*, 200.
(41) Becke, A. D. *J. Chem. Phys.* **1993**, *98*, 5648.
(42) Stephens, P. J.; Devlin, F. J.; Chablowski, C. F.; Frisch, M. J. *J. Phys. Chem.* **1994**, *98*, 11623.
(43) Hertwig, R. H.; Koch, W. *Chem. Phys. Lett.* **1997**, *268*, 345.
(44) Slater, J. C. *Phys. Rev.* **1951**, *81*, 385.
(45) Vosko, S. H.; Wilk, L.; Nusair, M. *Can. J. Phys.* **1980**, *58*, 1200.
(46) Tsuneda, T.; Hirao, K. *Chem. Phys. Lett.* **1997**, *268*, 510.
(47) Tsuneda, T.; Suzumura, T.; Hirao, K. *J. Chem. Phys.* **1999**, *110*, 10664.
(48) Benmelouka, M.; Messaoudi, S.; Furet, E.; Gautier, R.; Le Fur, E.; Pivan, J.-Y. *J. Phys. Chem. A* **2003**, *107*, 4122.
(49) Hartmann, M.; Clark, T.; van Eldik, R. *J. Phys. Chem. A* **1999**, *103*, 9899.
(50) Wachters, A. J. H. *J. Chem. Phys.* **1970**, *52*, 1033.
(51) Hay, P. J. *J. Chem. Phys.* **1977**, *66*, 4377.
(52) Schäfer, A.; Horn, H.; Ahlrichs, R. *J. Chem. Phys.* **1992**, *97*, 2571.
(53) Kirkwood, J. G. *J. Chem. Phys.* **1934**, *2*, 351.
(54) Onsager, L. *J. Am. Chem. Soc.* **1936**, *58*, 1486.
(55) Szafran, M.; Karelson, M. M.; Katritzky, A. R.; Koput, J.; Zerner, M. C. *J. Comput. Chem.* **1993**, *14*, 371.
(56) Tomasi, J.; Persico, M. *Chem. Rev.* **1994**, *94*, 2027.
(57) Hehre, W. J.; Stewart, R. F.; Pople, J. A. *J. Chem. Phys.* **1969**, *51*, 2657.
(58) Stebler-Röthlisberger, M.; Hummel, W.; Pittet, P.-A.; Bürgi, H.-B.; Ludi, A.; Merbach, A. E. *Inorg. Chem.* **1988**, *27*, 1358.
(59) Day, P. N.; Jensen, J. H.; Gordon, M. S.; Webb, S. P.; Stevens, W. J.; Krauss, M.; Garmer, D.; Basch, H.; Cohen, D. *J. Chem. Phys.* **1996**, *105*, 1968.
(60) Gordon, M. S.; Freitag, M. A.; Bandyopadhyay, P.; Jensen, J. H.; Kairys, V.; Stevens, W. J. *J. Phys. Chem. A* **2001**, *105*, 293.
(61) Car, R.; Parrinello, M. *Phys. Rev. Lett.* **1985**, *55*, 2471.
(62) Tuckerman, M.; Laasonen, K.; Sprik, M.; Parrinello, M. *J. Phys. Chem.* **1995**, *99*, 5749.
(63) Lynch, B. J.; Zhao, Y.; Truhlar, D. G. *J. Phys. Chem. A* **2003**, *107*, 1384.
(64) Rudolph, W. W.; Pye, C. C. *Phys. Chem. Chem. Phys.* **1999**, *1*, 4583.
(65) Boys, E. B.; Bernardi, F. *Mol. Phys.* **1970**, *19*, 553.
(66) Simon, S.; Duran, M.; Dannenberg, J. J. *J. Chem. Phys.* **1996**, *105*, 11024.
(67) Rassolov, V. A.; Pople, J. A.; Ratner, M. A.; Windus, T. L. *J. Chem. Phys.* **1998**, *109*, 1223.
(68) Dobbs, K. D.; Hehre, W. J. *J. Comput. Chem.* **1987**, *8*, 861.

(69) Shadhukhan, S.; Muñoz, D.; Adamo, C.; Scuseria, G. E. *Chem. Phys. Lett.* **1999**, *306*, 83.
(70) Pavese, M.; Chawla, S.; Lu, D.; Lobaugh, J.; Voth, G. A. *J. Chem. Phys.* **1997**, *107*, 7428.
(71) Ducommun, Y.; Zbinden, D.; Merbach, A. E. *Helv. Chim. Acta* **1982**, *65*, 1385.
(72) Yamaguchi, T.; Niihara, M.; Takamuku, T.; Wakita, H.; Kanno, H. *Chem. Phys. Lett.* **1997**, *274*, 485.
(73) Smirnow, P.; Wakita, H.; Yamaguchi, T. *J. Phys. Chem. B* **1998**, *102*, 4802.
(74) Rudolph, W. W.; Pye, C. C. *J. Phys. Chem. A* **2000**, *104*, 1627.
(75) Cox, H.; Akibo-Betts, G.; Wright, R. R.; Walker, N. R.; Curtis, S.; Duncombe, B.; Stace, A. J. *J. Am. Chem. Soc.* **2003**, *125*, 233.
(76) Perdew, J. P. *Phys. Rev. B* **1986**, *33*, 8822.
(77) Pasquarello, A.; Petri, I.; Salmon, P. S.; Parisel, O.; Car, R.; Tóth, É.; Powell, D. H.; Fischer, H. E.; Helm, L.; Merbach, A. E. *Science* **2001**, *291*, 856.
(78) Persson, I.; Persson, P.; Sandström, M.; Ullström, A.-S. *J. Chem. Soc., Dalton Trans.* **2002**, 1256.
(79) Benfatto, M.; D'Angelo, P.; Della Longa, S.; Pavel, N. V. *Phys. Rev. B* **2002**, *65*, 174205.
(80) Blumberger, J.; Bernasconi, L.; Tavernelli, I.; Vuilleumier, R.; Sprik, M. *J. Am. Chem. Soc.* **2004**, *126*, 3928.
(81) Schwenk, C. F.; Rode, B. M. *ChemPhysChem.* **2003**, *4*, 931.
(82) Schwenk, C. F.; Rode, B. M. *J. Chem. Phys.* **2003**, *119*, 9523.
(83) Eichkorn, K.; Treutler, O.; Öhm, H.; Häser, M.; Ahlrichs, R. *Chem. Phys. Lett.* **1995**, *240*, 283.
(84) Powell, D. H.; Furrer, P.; Pittet, P.-A.; Merbach, A. E. *J. Phys. Chem.* **1995**, *99*, 16622.
(85) Armunanto, R.; Schwenk, C. F.; Rode, B. M. *J. Phys. Chem. A* **2003**, *107*, 3132.
(86) Fulton, J. L.; Heald, S. M.; Badyal, Y. S.; Simonson, J. M. *J. Phys. Chem. A* **2003**, *107*, 4688.
(87) Dang, L. X.; Schenter, G. K.; Fulton, J. L. *J. Phys. Chem. B* **2003**, *107*, 14119.
(88) Schwenk, C. F.; Loeffler, H. H.; Rode, B. M. *J. Chem. Phys.* **2001**, *115*, 10808.
(89) Bakó, I.; Hutter, J.; Pálinkás, G. *J. Chem. Phys.* **2002**, *117*, 9838.
(90) Naor, M. M.; Nostrand, K. V.; Dellago, C. *Chem. Phys. Lett.* **2003**, *369*, 159.
(91) Rotzinger, F. P., work in progress.